Search for charged Higgs bosons in the H ± → tb decay channel in pp collisions at √s=8 TeV using the ATLAS detector

著者	The ATLAS collaboration, Hara Kazuhiko, Kim Shinhong(nobuhiro), Okawa Hideki, Sato Koji, Ukegawa Fumihiko
journal or publication title	Journal of high energy physics
volume	2016
number	3
page range	217
year	2016-03
権利	Open Access, Copyright CERN, for the benefit of the ALICE Collaboration. Article funded by SCOAP3.
URL	http://hdl.handle.net/2241/00142106

Published for SISSA by Springer

Received: December 14, 2015
Revised: February 1, 2016
Accepted: February 2, 2016
Published: March 17, 2016

Search for charged Higgs bosons in the $H^{\pm} \to tb$ decay channel in pp collisions at $\sqrt{s} = 8\,\text{TeV}$ using the ATLAS detector

The ATLAS collaboration

E-mail: atlas.publications@cern.ch

Abstract: Charged Higgs bosons heavier than the top quark and decaying via $H^{\pm} \to tb$ are searched for in proton-proton collisions measured with the ATLAS experiment at $\sqrt{s} = 8\,\text{TeV}$ corresponding to an integrated luminosity of $20.3\,\text{fb}^{-1}$. The production of a charged Higgs boson in association with a top quark, $gb \to tH^{\pm}$, is explored in the mass range 200 to 600 GeV using multi-jet final states with one electron or muon. In order to separate the signal from the Standard Model background, analysis techniques combining several kinematic variables are employed. An excess of events above the background-only hypothesis is observed across a wide mass range, amounting to up to 2.4 standard deviations. Upper limits are set on the $gb \to tH^{\pm}$ production cross section times the branching fraction BR($H^{\pm} \to tb$). Additionally, the complementary s-channel production, $qq' \to H^{\pm}$, is investigated through a reinterpretation of $W' \to tb$ searches in ATLAS. Final states with one electron or muon are relevant for $H^{\pm}$ masses from 0.4 to 2.0 TeV, whereas the all-hadronic final state covers the range 1.5 to 3.0 TeV. In these search channels, no significant excesses from the predictions of the Standard Model are observed, and upper limits are placed on the $qq' \to H^{\pm}$ production cross section times the branching fraction BR($H^{\pm} \to tb$).

Keywords: Hadron-Hadron scattering, Higgs physics

ArXiv ePrint: 1512.03704

doi:10.1007/JHEP03(2016)127

JHEP03(2016)127

Contents

JHEP03(2016)127

1 Introduction

The discovery of a neutral scalar particle H at the Large Hadron Collider (LHC) in 2012 [1, 2], with a measured mass of $125.09 \pm 0.21(\text{stat.}) \pm 0.11(\text{syst.})$ GeV [3], raises the question of whether this new particle is the Higgs boson of the Standard Model (SM) or one physical state of an extended Higgs sector. The observation of a heavy charged scalar particle would clearly indicate physics beyond the SM. Charged Higgs bosons[1] are predicted by several non-minimal Higgs scenarios, such as two-Higgs-doublet Models (2HDM) [4] and models containing Higgs triplets [5–9].

The production mechanisms and decay modes of a charged Higgs boson depend on its mass, m_{H^+}. For light charged Higgs bosons ($m_{H^+} \lesssim m_{\text{top}}$, where m_{top} is the top-quark mass), the primary production mechanism is through the decay of a top quark, $t \to bH^+$. For $m_{H^+} > m_{\text{top}}$, the dominant H^+ production mode at the LHC is expected to be in association with a top quark, as illustrated by the left-hand and central plots

[1] In the following, charged Higgs bosons are denoted H^+, with the charge-conjugate H^- always implied. Similarly, generic quark symbols are used for q and $\bar{q}$.

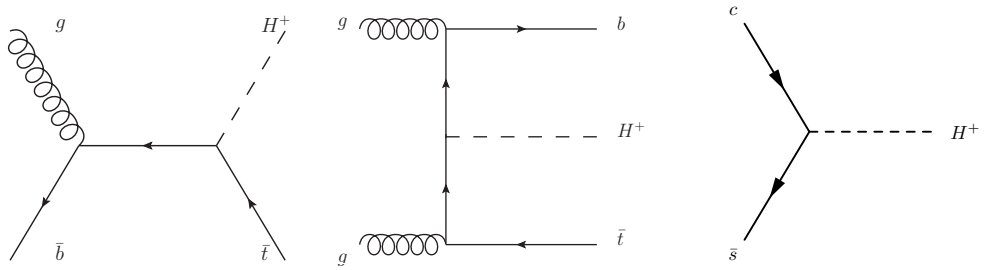

Figure 1. Leading-order Feynman diagrams for the production of a charged Higgs boson with a mass $m_{H^+} > m_{\text{top}}$, in association with a top quark (left in the 5FS, and centre in the 4FS) and in the s-channel (right).

of figure 1. When calculating the corresponding cross section in a four-flavour scheme (4FS), b-quarks are dynamically produced, whereas in a five-flavour scheme (5FS), the b-quark is also considered as an active flavour inside the proton. The 4FS and 5FS cross sections are averaged according to ref. [10]. In the 2HDM, the production and decay of the charged Higgs boson also depend on the parameter $\tan\beta$, defined as the ratio of the vacuum expectation values of the two Higgs doublets, and the mixing angle α between the CP-even Higgs bosons. For $m_{H^+} > m_{\text{top}}$ and in the case of $\cos(\beta-\alpha) \approx 0$, the dominant decay is $H^+ \to tb$, with a substantial contribution from $H^+ \to \tau\nu$ for large values of $\tan\beta$ [11]. A complementary H^+ production mode, shown in the right-hand plot of figure 1, is the s-channel process, $qq' \to H^+$.

The LEP experiments placed upper limits on the production of H^+ in the mass range of 40–100 GeV [12], and the Tevatron experiments set upper limits on $\text{BR}(t \to bH^+)$ for m_{H^+} in the range 80–150 GeV [13, 14]. The D0 experiment also searched for a charged Higgs boson with a mass in the range 180–300 GeV using the $H^+ \to tb$ decay channel [15]. Light charged Higgs bosons have been searched for in the $\tau\nu$ decay mode at the LHC by CMS (2 fb^{-1}, $\sqrt{s} = 7$ TeV [16]) and ATLAS (4.7 fb^{-1}, $\sqrt{s} = 7$ TeV [17, 18]). Searches for charged Higgs bosons were also performed in proton-proton (pp) collisions at $\sqrt{s} = 8$ TeV, by ATLAS using the $\tau\nu$ decay mode [19] and by CMS using final states originating from both the $\tau\nu$ and tb decay modes [20]. CMS set an upper limit of 2.0–0.13 pb on the production cross section times branching fraction for $H^+ \to tb$ in the mass range 180–600 GeV. Vector-boson-fusion H^+ production was also searched for by ATLAS using the WZ final state [21]. No evidence for a charged Higgs boson was found in any of these searches.

This paper describes searches for charged Higgs bosons decaying into tb. In the H^+ mass range of 200–600 GeV, the production mode in association with a top quark is studied. The 5FS process is generated. Cross sections averaging 4FS and 5FS are used for model-dependent predictions. The search is based on selecting two top quarks, with their decays producing one charged lepton (electron or muon), and at least one additional jet containing a b-flavoured hadron. In the complementary s-channel production mode, H^+ masses between 0.4 and 2.0 TeV are explored in a final state containing one charged lepton and jets (referred to as lepton+jets in the following), while the all-hadronic final state is

JHEP03(2016)127

used for very high H^+ masses, 1.5 to 3.0 TeV, with a jet substructure technique to reconstruct the top-quark decay products in one single large-radius jet. The two s-channel analyses are reinterpretations of recent searches for $W' \to tb$ in ATLAS [22, 23]. Based on dedicated simulations of the $H^+ \to tb$ signal and a reinterpretation of the data, upper limits are derived for the s-channel production of a charged scalar particle decaying to tb.

The paper is organised as follows. Section 2 describes briefly the ATLAS detector, then summarises the data and the samples of simulated events used for the analyses. Section 3 describes the reconstruction of objects in ATLAS. Section 4 presents the event selection and analysis strategy of the search for $H^+ \to tb$ produced in association with a top quark. Systematic uncertainties are also discussed, before exclusion limits in terms of cross section times branching fraction are presented, together with their interpretation in benchmark scenarios of the Minimal Supersymmetric Standard Model (MSSM) [24–28]. The reinterpretations of $W' \to tb$ analyses as searches for the production of $H^+ \to tb$ in the s-channel, including a discussion of the H^+ signal shapes and uncertainties, are presented in section 5. Finally, a summary is given in section 6.

2 Data and simulated events

2.1 ATLAS detector and data sample

The ATLAS detector [29] consists of an inner tracking system with coverage in pseudorapidity[2] up to $|\eta| = 2.5$, surrounded by a thin 2 T superconducting solenoid, a calorimeter system extending up to $|\eta| = 4.9$ and a muon spectrometer extending up to $|\eta| = 2.7$ that measures the deflection of muon tracks in the field of three superconducting toroid magnets. A three-level trigger system is used to select events of interest. The first-level trigger (L1) is implemented in hardware, using a subset of detector information to reduce the event rate to no more than 75 kHz. This is followed by two software-based trigger levels (L2 and EF), which together further reduce the event rate to less than 400 Hz.

Stringent data-quality requirements are applied, resulting in an integrated luminosity of 20.3 fb^{-1} for the 2012 data-taking period. The integrated luminosity has an uncertainty of 2.8%, measured following the methodology described in ref. [30]. Events are required to have a primary vertex with at least five associated tracks, each with a transverse momentum p_{T} greater than 400 MeV. If an event has more than one reconstructed vertex satisfying these criteria, the primary vertex is defined as the reconstructed vertex with the largest sum of squared track transverse momenta.

2.2 Background and signal modelling

The background processes for the searches in this paper include SM pair production of top quarks (with additional jets, or in association with a vector boson $V = W, Z$ or the SM

[2] ATLAS uses a right-handed coordinate system with its origin at the nominal interaction point (IP) in the centre of the detector and the z-axis along the beam pipe. The x-axis points from the IP to the centre of the LHC ring, and the y-axis points upwards. Cylindrical coordinates (r, ϕ) are used in the transverse plane, ϕ being the azimuthal angle around the z-axis. The pseudorapidity is defined in terms of the polar angle θ as $\eta = -\ln\tan(\theta/2)$.

JHEP03(2016)127

Higgs boson), as well as the production of single-top-quark, W+jets, Z/γ^*+jets, diboson ($WW/WZ/ZZ$) and multi-jet events. The dominant background is the production of $t\bar{t}$ pairs with additional jets in the final state.

In the analyses with an electron or a muon in the final state, all backgrounds are taken from simulation, except for the multi-jet events. These mostly contribute via the presence of a non-prompt electron or muon, e.g. from a semileptonic b- or c-flavoured hadron decay, or through the misidentification of a jet. The normalisation of the multi-jet events and the shape of the relevant distributions are determined with a data-driven technique known as the matrix method [31]. In the search for $H^+ \to tb$ in the s-channel production mode with an all-hadronic final state, all backgrounds are estimated using a data-driven method based on a combined fit to the data under the SM background plus H^+ signal hypothesis.

The modelling of $t\bar{t}$ events is performed with Powheg-Box v2.0 [32, 33], using the CT10 [34, 35] parton distribution function (PDF) set. It is interfaced to Pythia v6.425 [36], with the Perugia P2011C [37] set of tuned parameters (tune) for the underlying event. The $t\bar{t}$ cross section at 8 TeV is $\sigma_{t\bar{t}} = 253^{+13}_{-15}$ pb for a top-quark mass of 172.5 GeV. It is calculated at next-to-next-to-leading order (NNLO) in QCD including resummation of next-to-next-to-leading logarithmic (NNLL) soft gluon terms with Top++ v2.0 [38–44].

In the search for H^+ production in association with a top quark, simulated $t\bar{t}$ events are classified according to their flavour content at parton level, using the same methodology as in ref. [45]. Events are labelled as $t\bar{t}$+$b\bar{b}$ if they contain at least one particle jet that is matched to a b-flavoured hadron not originating from the decay of the $t\bar{t}$ system. Events where at least one particle jet is matched to a c-flavoured hadron, and not already labelled as $t\bar{t}$+$b\bar{b}$, are labelled as $t\bar{t}$+$c\bar{c}$. Events labelled as either $t\bar{t}$+$b\bar{b}$ or $t\bar{t}$+$c\bar{c}$ are generically referred to as $t\bar{t}$+heavy-flavour (HF) events. The remaining events, including those with no additional jets, are labelled as $t\bar{t}$+light-flavour (LF). In the following, a sequential reweighting is applied at the generator level for all $t\bar{t}$+LF and $t\bar{t}$+$c\bar{c}$ events produced with Powheg+Pythia. Two correction factors are used, based on the values of the transverse momenta of the top quark and the $t\bar{t}$ system, taking the correlation between these two parameters into account. This reweighting procedure was originally implemented in order to match simulation to data in the measurement of top-quark-pair differential cross sections at $\sqrt{s} = 7$ TeV [46]. It was verified that this procedure is also reasonable at $\sqrt{s} = 8$ TeV. The $t\bar{t}$+$b\bar{b}$ component is reweighted to match the NLO theory calculation provided within Sherpa with the OpenLoops framework [47, 48]. For this reweighting, the same settings as in ref. [45] are used in this paper. The reweighting is performed at the generator level using several kinematic variables such as the transverse momenta of the top quark, the $t\bar{t}$ system and the dijet system not coming from the top-quark decay, as well as the distance[3] ΔR_{jj} between these two jets. For systematic studies, an alternative $t\bar{t}$+jets sample is generated with the Madgraph5 v1.5.11 LO generator [49], using the CT10 PDF set and interfaced to Pythia v6.425 for parton shower and fragmentation.

Samples of $t\bar{t}V$ events are generated using Madgraph5 v1.3.33, with the CTEQ6L1 [50] PDF, interfaced to Pythia v6.425 for the showering and hadronisation, with the AUET2B

[3] $\Delta R = \sqrt{(\Delta\eta)^2 + (\Delta\phi)^2}$, where $\Delta\eta$ is the difference in pseudorapidity of the two objects in question, and $\Delta\phi$ is the difference between their azimuthal angles.

JHEP03(2016)127

underlying-event tune [51]. They are normalised to the next-to-leading-order (NLO) cross section [52, 53].

Single-top-quark production in the s- and Wt-channels are simulated with POWHEG-BOX v2.0, using the CT10 PDF, interfaced to PYTHIA v6.425 with the underlying-event tune P2011C. The same procedure is used for the single-top-quark production in the t-channel, except in the search for $qq' \to H^+ \to tb$ in the lepton+jets final state, where the leading-order (LO) generator ACERMC v3.8 [54] with the CTEQ6L1 PDF, interfaced to PYTHIA v6.425 with the underlying-event tune P2011C, is used instead. Overlaps between the $t\bar{t}$ and Wt final states are handled using inclusive diagram removal [55]. The single-top-quark samples are normalised to the approximate NNLO theoretical cross sections [56–58] using the MSTW2008 NNLO [59–61] PDF.

Samples of W/Z+jets events are generated using the ALPGEN v2.14 [62] generator, with the CTEQ6L1 PDF, interfaced to PYTHIA v6.425 with the underlying-event tune P2011C. The W+jets events are generated with up to five additional partons, separately for the W+LF, $Wb\bar{b}$+jets, $Wc\bar{c}$+jets and Wc+jets processes. Similarly, the Z+jets background is generated with up to five additional partons separated in different flavours. The samples of W/Z+jets events are normalised to the inclusive NNLO theoretical cross sections [63]. Finally, the W/Z+jets events are reweighted to account for differences in the W/Z p_{T} spectrum between data and simulation [64].

In the searches for $H^+ \to tb$ with a lepton+jets final state, diboson events are generated with the requirement of having at least one boson decaying leptonically. ALPGEN v2.14 is used, with the CTEQ6L1 PDF, and it is interfaced to HERWIG v6.520 [65] for showering and hadronisation, together with JIMMY v4.31 [66] for the underlying event, using the AUET2 tune [67]. The diboson backgrounds are normalised to the production cross sections calculated at NLO [68].

The production of the SM Higgs boson in association with a top-quark pair ($t\bar{t}H$) is modelled using NLO matrix elements obtained from the HELAC-ONELOOP package [69]. POWHEG-BOX is used as an interface to shower simulation programs. The samples created using this approach are referred to as POWHEL samples [70]. They are inclusive in Higgs boson decays and are produced for a Higgs boson mass of 125 GeV, using the CT10 PDF, and interfaced to PYTHIA v8.1 [71] with the AU2 underlying-event tune [72]. As in the generation of $t\bar{t}$ background events, the top-quark mass is set to 172.5 GeV. The $t\bar{t}H$ cross section and the decay branching fractions of the Higgs boson are taken from the (N)NLO theoretical calculations collected in ref. [73].

In the search for H^+ produced in association with a top quark, signal samples are generated with POWHEG-BOX, using the CT10 PDF, interfaced to PYTHIA v8.1 with the AU2 underlying-event tune. For the m_{H^+} range of 200–300 GeV, the samples are produced in steps of 25 GeV, then in intervals of 50 GeV up to 600 GeV. The samples are generated at NLO using the 5FS and with a zero width for H^+.

In the search for H^+ in the s-channel, signal events are generated using MADGRAPH5 v1.5.12, with the CTEQ6L1 PDF, interfaced to PYTHIA v8.1 with the AU2 underlying-event tune, for both the lepton+jets and all-hadronic final states. In the former (latter) case, samples are produced in m_{H^+} steps of 200 (250) GeV, between 0.4 and 2.0 TeV (1.5

JHEP03(2016)127

and 3.0 TeV). A narrow-width approximation is used for both final states. This is justified as the experimental resolution is much larger than the H^+ natural width.

In all background simulations, TAUOLA v1.20 [74] is used for the τ decays and PHOTOS v2.15 [75] is employed for photon radiation from charged leptons. For the signal simulations, PHOTOS++ v3.51 [76] is used. All signal and background events are overlaid with additional minimum-bias events generated using PYTHIA v8.1 with the MSTW2008 LO PDF and the AUET2 underlying-event tune, in order to simulate the effect of multiple pp collisions per bunch crossing (pile-up). Finally, all background samples and all-hadronic signal samples are processed through a simulation [77] of the detector geometry and response using GEANT4 [78]. The signal samples with leptons in the final state are passed through a fast simulation of the calorimeter response [79]. All samples from simulation are processed through the same reconstruction software as the data.

3 Object reconstruction and identification

The main objects used for the searches reported in this paper are electrons, muons, jets (possibly identified as originating from b-quarks), and missing transverse momentum. A brief summary of the main reconstruction and identification criteria used for each of these objects is given below.

Electron candidates [80] are reconstructed from energy deposits (clusters) in the electromagnetic calorimeter which are associated with a reconstructed track in the inner detector system. Their transverse energy, $E_{\mathrm{T}} = E_{\mathrm{clus}}/\cosh(\eta_{\mathrm{track}})$, is computed using the electromagnetic cluster energy E_{clus} and the direction of the electron track η_{track}, and is required to exceed 25 GeV. The pseudorapidity range for the electromagnetic cluster covers the fiducial volume of the detector, $|\eta| < 2.47$ (the transition region between the barrel and end-cap calorimeters, $1.37 < |\eta| < 1.52$, is excluded). The longitudinal impact parameter $|z_0|$ of the electron track relative to the primary vertex must be smaller than 2 mm. In order to reduce the contamination from misidentified hadrons, electrons from heavy-flavour decays and photon conversions, the electron candidates are also required to satisfy E_{T}- and η-dependent calorimeter (and tracker) isolation requirements imposed in a cone with a fixed size $\Delta R = 0.2$ (0.3) around the electron position.

Muon candidates are reconstructed from track segments in the muon spectrometer, and matched with tracks found in the inner detector system [81]. The final muon candidates are refitted using the complete track information from both detector systems, and they are required to satisfy $p_{\mathrm{T}} > 25$ GeV, $|\eta| < 2.5$ and $|z_0| < 2$ mm. Furthermore, muons must fulfil a p_{T}-dependent track-based isolation requirement that has good performance under high pile-up conditions and/or when the muon is close to a jet. For that purpose, the scalar sum of the track p_{T} in a cone of a variable size, defined by $\Delta R = 10\,\mathrm{GeV}/p_{\mathrm{T}}$, around the muon position (while excluding the muon track itself) must be less than 5% of the muon transverse momentum.

Jets are reconstructed from topological energy clusters [82] in the calorimeters, using the anti-k_t algorithm [83, 84]. Two radius parameters are used, $R = 0.4$ ('small-radius jets') or $R = 1.0$ ('large-radius jets'). The large-radius jets are only used when recon-

JHEP03(2016)127

structing high-p_{T} top quarks as single objects in the search for $H^+ \to tb$ produced in the s-channel and decaying into an all-hadronic final state, as described below. When no jet type is specified, small-radius jets are implied. Small- and large-radius jets are calibrated using energy- and η-dependent correction factors derived from simulation and with residual corrections from in situ measurements [85]. Only small-radius jets that have $p_{\mathrm{T}} > 25\,\mathrm{GeV}$ and $|\eta| < 2.5$ are considered in this paper. Jets originating from pile-up interactions are suppressed by requiring that at least 50% of the scalar sum of the p_{T} of the associated tracks is due to tracks originating from the primary vertex [86]. This is referred to as the jet vertex fraction (JVF) and is only applied to jets with $p_{\mathrm{T}} < 50\,\mathrm{GeV}$ and $|\eta| < 2.4$.

Jets are identified as originating from the hadronisation of a b-quark (b-tagged) via an algorithm that uses multivariate techniques to combine information from the impact parameters of displaced tracks with topological properties of secondary and tertiary decay vertices reconstructed within the jet [87]. The nominal working point used here is chosen to correspond to a 70% efficiency to tag a b-quark jet, with a light-jet mistag rate of 1% and a c-jet mistag rate of 20%, as determined with b-tagged jets with $p_{\mathrm{T}} > 20\,\mathrm{GeV}$ and $|\eta| < 2.5$ in simulated $t\bar{t}$ events. The tagging efficiencies from simulation are corrected based on the results of flavour-tagging calibrations performed with the data [88].

In the search for $H^+ \to tb$ produced in the s-channel and decaying into an all-hadronic final state (section 5.2), hadronically decaying high-p_{T} top quarks are reconstructed as single objects through 'top-tagging'. Large-radius jets are used as input to the top-tagger. In order to minimise the effects of pile-up [89], the large-radius jets are trimmed [90]. The trimming is performed by reclustering the large-radius jet using the inclusive k_t algorithm [91] with a jet radius parameter $R = 0.3$, and by removing soft subjets with a p_{T} smaller than 5% of the original jet p_{T}. Trimmed large-radius jets are required to have $p_{\mathrm{T}} > 350\,\mathrm{GeV}$ and $|\eta| < 2.0$. Large-radius jets are top-tagged if they have a substructure compatible with a three-prong decay. The top-tagger used in the search of section 5.2 was developed for the search for $W' \to tb$ in ATLAS [23]. It uses the k_t splitting scale [91] $\sqrt{d_{12}}$ and the N-subjettiness [92, 93] variables τ_{21} and τ_{32}. The k_t algorithm clusters the hardest objects last, which means that a two-body decay (such as $t \to bW$) typically gets a larger value of $\sqrt{d_{12}}$ than light jets. The τ_{ij} distribution peaks closer to 0 for i-subjet-like jets and closer to 1 for j-subjet-like jets. The top-tagged jet is required to pass the cuts $\sqrt{d_{12}} > 40\,\mathrm{GeV}$, $\tau_{32} < 0.65$, and $0.4 < \tau_{21} < 0.9$, as in the search for $W' \to tb$ [23].

When several selected objects overlap geometrically, the following procedures are applied. In the searches with a lepton+jets final state, muons are rejected if found to be $\Delta R < 0.4$ from any jet with nominal p_{T}, η and JVF selections. In order to avoid double-counting of electrons as jets, the closest jet to an electron is then removed if lying $\Delta R < 0.2$ from an electron. Finally, electrons are rejected if found to be $\Delta R < 0.4$ from any remaining jet with nominal p_{T}, η and JVF selections. In the search for s-channel production of $H^+ \to tb$ in the all-hadronic final state, large-radius jets are required to be separated by $\Delta R > 2.0$ from the small-radius b-tagged jets used to reconstruct the invariant mass of H^+ candidates. Events with electrons (muons) fulfilling $E_{\mathrm{T}} > 30\,\mathrm{GeV}$ ($p_{\mathrm{T}} > 30\,\mathrm{GeV}$) are vetoed in this particular search channel.

The magnitude $E_{\mathrm{T}}^{\mathrm{miss}}$ of the missing transverse momentum is reconstructed from the negative vector sum of transverse momenta of reconstructed objects, as well as from un-

JHEP03(2016)127

matched topological clusters and tracks (collected in a so-called soft term). The $E_{\mathrm{T}}^{\mathrm{miss}}$ is further refined by using object-level corrections for the identified electrons, muons and jets, and the effects of pile-up in the soft term are mitigated [94].

4 Search for a charged Higgs boson in association with a top quark

4.1 Event selection and categorisation

In this section, the search for a charged Higgs boson produced in association with a top quark, $gb \to tH^+$ with $H^+ \to tb$, is described. In the events selected for this analysis, the top quarks both decay via $t \to Wb$, where one W boson decays hadronically and the other decays into an electron or a muon, either directly or through a τ-lepton decay, and the corresponding neutrino(s). The signal event signature is therefore characterised by the presence of exactly one high-p_{T} charged lepton (electron or muon) and five or more jets, at least three of them being b-tagged.

Events collected using either an isolated or non-isolated single-lepton trigger are considered. Isolated triggers have a threshold of 24 GeV on p_{T} for muons and on E_{T} for electrons, while non-isolated triggers have higher thresholds at 36 GeV (muons) and 60 GeV (electrons). The isolated triggers have a loss of efficiency at high p_{T} or E_{T}, which is recovered by the triggers with higher thresholds. Events accepted by the trigger are then required to have exactly one identified electron or muon, and at least four jets, of which at least two must be identified as b-tagged jets. The selected lepton is required to match, with $\Delta R < 0.15$, a lepton reconstructed by the trigger.

At this stage, the samples contain mostly $t\bar{t}$ events. The selected events are further categorised into different regions, depending on the number of jets and b-tagged jets. The categories are inclusive in the lepton flavour. In the following, a given category with m jets, of which n are b-tagged, is referred to as mj(nb). A total of five independent categories are considered: four control regions (CR) with little sensitivity to signal, 4j(2b), 5j(2b), $\geq$6j(2b), 4j($\geq$3b), and one signal-rich region (SR), $\geq$5j($\geq$3b). The CR are used to control the backgrounds and to constrain systematic uncertainties (section 4.3). For each category, the expected event yields of all processes and the number of events observed in the data are given in table 1. The dominant background process in every category is $t\bar{t}$+LF. In the signal-rich region, contributions from $t\bar{t}$+HF are also sizeable. In all categories except $\geq$6j(2b), the data exceed the SM prediction, but they are consistent within the large uncertainties on the background. In table 2, the expected amount of signal is listed for a few points of the $m_h^{\mathrm{mod}-}$ benchmark scenario of the MSSM [95]. The theoretical predictions are taken from refs. [11, 96–98].

4.2 Analysis strategy

In order to separate the H^+ signal from the SM background, and to constrain the large uncertainties on the background, different discriminants are used depending on the event category, and are then combined in a binned maximum-likelihood fit. In the four CR, the discriminating variable is the scalar sum of the p_{T} of the selected jets ($H_{\mathrm{T}}^{\mathrm{had}}$) and

JHEP03(2016)127

Process	4j(2b)	5j(2b)	≥6j(2b)	4j(≥3b)	≥5j(≥3b)
$t\bar{t}$+LF	80 300 ± 9900	38 700 ± 7400	19 300 ± 5300	6300 ± 1000	5600 ± 1600
$t\bar{t}$+$c\bar{c}$	5200 ± 2900	4500 ± 2600	3800 ± 2300	740 ± 410	1800 ± 1000
$t\bar{t}$+$b\bar{b}$	1720 ± 940	1550 ± 830	1390 ± 820	660 ± 370	2300 ± 1200
$t\bar{t}H$	33.7 ± 4.6	44.6 ± 5.4	68.9 ± 9.1	15.5 ± 2.5	87 ± 11
$t\bar{t}V$	128 ± 40	151 ± 47	189 ± 59	17.6 ± 5.7	85 ± 27
Single-top	5020 ± 770	1970 ± 420	880 ± 270	360 ± 83	330 ± 110
W+jets	3400 ± 1700	1270 ± 720	640 ± 400	190 ± 100	170 ± 100
Z+jets	1330 ± 670	400 ± 220	150 ± 95	53 ± 31	49 ± 39
VV	232 ± 69	108 ± 41	52 ± 25	10.7 ± 3.6	13.7 ± 6.0
Multi-jets	2160 ± 870	670 ± 260	330 ± 150	160 ± 67	150 ± 100
Total bkg	100 000 ± 11 000	49 300 ± 8600	27 100 ± 6600	8500 ± 1300	10 600 ± 2500
Data	102 462	51 421	26 948	9102	11 945

Table 1. Expected event yields of the SM background processes and observed data in the five categories. The first four columns show the event yields in the CR, the last column shows the event yields in the SR. The uncertainties include statistical and systematic components (systematic uncertainties are discussed in section 4.3).

m_{H^+} [GeV]	$\tan\beta$	4j(2b)	5j(2b)	≥6j(2b)	4j(≥3b)	≥5j(≥3b)
200	0.5	2580 ± 420	1670 ± 190	1050 ± 300	730 ± 190	1750 ± 200
	0.7	1290 ± 210	834 ± 93	520 ± 150	366 ± 95	880 ± 100
	0.9	760 ± 120	493 ± 55	309 ± 88	216 ± 56	518 ± 59
400	0.5	397 ± 69	406 ± 44	390 ± 100	211 ± 56	756 ± 76
	0.7	200 ± 35	204 ± 22	197 ± 51	106 ± 28	380 ± 38
	0.9	119 ± 21	121 ± 13	117 ± 31	63 ± 17	226 ± 23
600	0.5	71 ± 14	85 ± 12	107 ± 29	36 ± 11	183 ± 23
	0.7	34.7 ± 6.9	41.5 ± 5.6	52 ± 14	17.4 ± 5.3	89 ± 11
	0.9	19.8 ± 3.9	23.7 ± 3.2	29.8 ± 8.1	10.0 ± 3.0	50.9 ± 6.5

Table 2. Number of expected signal events in the five categories for a few representative points of the $m_h^{\text{mod}-}$ scenario of the MSSM. The last column shows the event yields in the SR. The expected uncertainties contain statistical and systematic components (systematic uncertainties are discussed in section 4.3). Uncertainties on the cross sections and branching fractions for the $m_h^{\text{mod}-}$ scenario are not included.

in the SR, the output of a boosted decision tree (BDT) is used. The Toolkit for Multivariate Data Analysis (TMVA) [99] is used for the training and evaluation of the BDT responses. The BDT is trained to specifically discriminate the H^+ signal from the $t\bar{t}$+$b\bar{b}$ background process. This method reduces correlations and anti-correlations between the signal normalisation and the parameters connected to the dominant systematic uncertainties, in particular for H^+ masses below 350 GeV, where those correlations are sizeable. The largest correlation at low mass is that between the $t\bar{t}$+$b\bar{b}$ cross section and the signal normalisation, which is −50% at 200 GeV. Consequently, this specific BDT is more sensitive than a BDT trained against the sum of all backgrounds when uncertainties are included.

JHEP03(2016)127

The variables entering the BDT training are:

- the scalar sum of the p_{T} of all selected jets ($H_{\mathrm{T}}^{\mathrm{had}}$),
- the p_{T} of the leading jet,
- the invariant mass of the two b-tagged jets that are closest in ΔR,
- the second Fox-Wolfram moment [100], calculated from the selected jets,
- the average ΔR between all pairs of b-tagged jets in the event.

Many other kinematic and event shape variables were tested before this set of variables was selected. The variables listed above provide the best separation between signal and background across all mass hypotheses. The BDT training is performed independently for each H^+ mass hypothesis, and only for events in the SR. The BDT input variables were validated in the CR by comparing their distributions in the data and simulation, and they were further validated by evaluating the BDT responses in the four CR for every mass point. The data and expected SM backgrounds were found to be compatible at all times. The statistical analysis was performed after the selection and the BDT training were finalised.

The pre-fit distributions of $H_{\mathrm{T}}^{\mathrm{had}}$ in the four control regions are displayed in figure 2. Good agreement between data and the SM expectation is found, given the large uncertainties. The pre-fit BDT output distributions for two mass hypotheses are shown in figure 3. In the SR, the data exceed the expected background, but they are consistent given the large uncertainties. The discrimination between signal and background significantly improves for larger signal masses.

4.3 Systematic uncertainties

Several sources of systematic uncertainty, affecting the normalisation of signal and background processes or the shape of their distributions, are considered. The individual sources of systematic uncertainty are assumed to be uncorrelated, but correlations of a given systematic effect are maintained across categories and processes, when applicable. All variations, except those from uncertainties on the theoretical cross section, are symmetrised with respect to the nominal value. The uncertainties arising from the reconstructed objects and the background modelling, in particular the $t\bar{t}$ background modelling, receive the same treatment as in ref. [45].

The following uncertainties on the reconstructed objects are considered. The systematic uncertainties associated with the electron or muon selection arise from the trigger, reconstruction and identification efficiency, isolation criteria, as well as from the momentum scale and resolution [80, 81]. In total, the systematic uncertainties associated with electrons (muons) include five (six) components. The systematic uncertainties associated with the jet selection arise from the jet energy scale (JES), the JVF requirement, the jet energy resolution and the jet reconstruction efficiency. Among these, the JES uncertainty has the largest impact on the search. It is derived by combining information from test-beam

JHEP03(2016)127

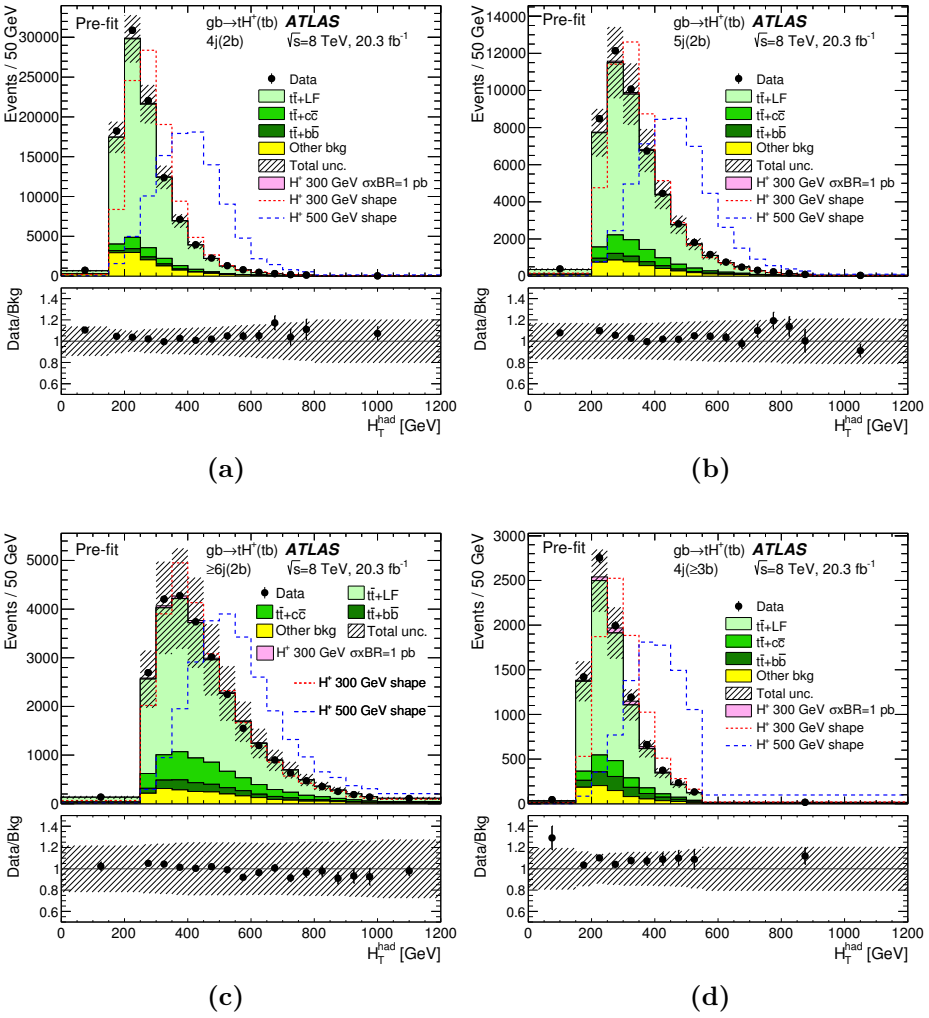

Figure 2. Pre-fit distributions of the scalar sum of the p_{T} of all selected jets, $H_{\mathrm{T}}^{\mathrm{had}}$, for the four control regions: (a) 4j(2b), (b) 5j(2b), (c) ≥6j(2b), (d) 4j(≥3b). Each background process is normalised according to its cross section. A signal with $m_{H^+} = 300\,\mathrm{GeV}$, normalised to a production cross section times branching fraction for $H^+ \to tb$ ($\sigma \times \mathrm{BR}$) of 1 pb, is shown in pink, stacked on top of the background. Two signal shapes are shown superimposed as dashed lines normalised to the data. The last bin includes the overflow. The hatched bands show the pre-fit uncertainties, which are dominated by systematic uncertainties (discussed in section 4.3). The lower panels display the ratio of the data to the total predicted background.

data, LHC collision data and simulation [85]. The JES uncertainty is split into 22 uncorrelated sources, which can have different jet p_{T}- and η-dependencies. Six (four) independent sources of systematic uncertainty affecting the $b(c)$-tagging efficiency are considered [88]. An additional uncertainty is assigned due to the extrapolation of the measurement of the b-tagging efficiency to the high-p_{T} region. Twelve uncertainties are considered for the light-jet mistagging rate, with dependencies on the jet p_{T} and η.

The uncertainty on the inclusive $t\bar{t}$ production cross section is $+5\%/-6\%$ [38–44]. It accounts for uncertainties from the choice of PDF, α_{S} and the top-quark mass. The

JHEP03(2016)127

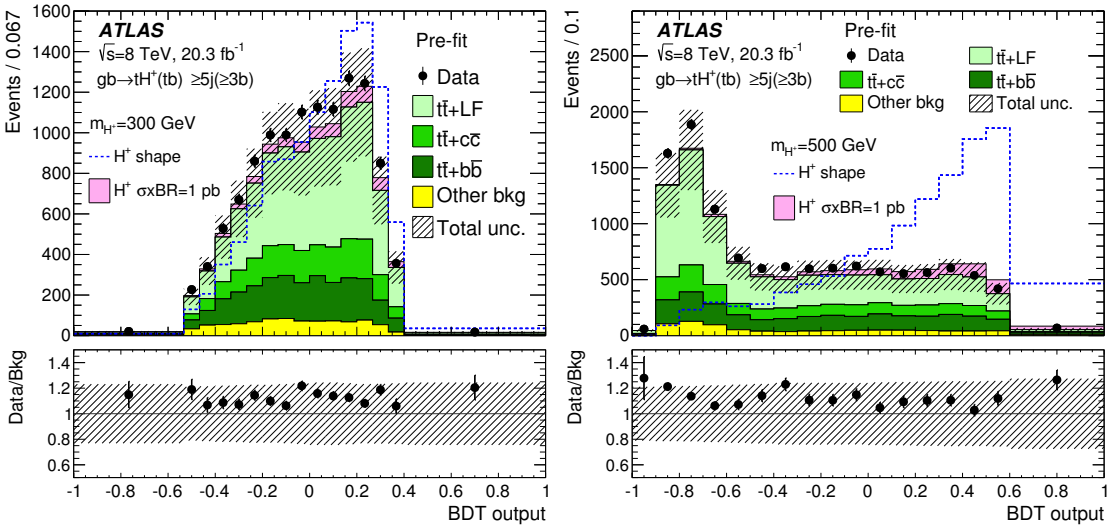

(a) **(b)**

Figure 3. Pre-fit distributions of the BDT output in the signal-rich region trained for two signal mass hypotheses: (a) 300 GeV and (b) 500 GeV. Each background process is normalised according to its cross section. A signal, normalised to a production cross section times branching fraction for $H^+ \to tb$ ($\sigma \times \mathrm{BR}$) of 1 pb, is shown in pink, stacked on top of the background. The signal shape is shown superimposed as dashed line normalised to the data. The hatched bands show the pre-fit uncertainties, which are dominated by systematic uncertainties (discussed in section 4.3). The lower panels display the ratio of the data to the total predicted background.

PDF and α_S uncertainties were calculated using the PDF4LHC prescription [101] with the MSTW2008 68% CL NNLO, CT10 NNLO and NNPDF2.3 NNLO [102] PDF sets, added in quadrature to the scale uncertainty. Systematic uncertainties due to the choice of parton shower and hadronisation models are derived by comparing $t\bar{t}$ events produced with Powheg-Box interfaced to either Pythia or Herwig. Nine uncertainties associated with the experimental measurement of the p_T of the top quark and the $t\bar{t}$ system are considered as separate sources of systematic uncertainty in the reweighting procedure [46]. Two additional uncorrelated uncertainties are assigned specifically to $t\bar{t}$+$c\bar{c}$ events, consisting of the full difference between applying and not applying the p_T reweighting procedure for the top quark and the $t\bar{t}$ system, respectively. A conservative systematic uncertainty of 50% is applied to $t\bar{t}$+$b\bar{b}$ events to account for differences between the cross sections obtained with Powheg+Pythia and the NLO prediction based on Sherpa with OpenLoops [47, 48]. In the absence of an NLO prediction for $t\bar{t}$+$c\bar{c}$, the same uncertainty of 50% is applied to this component of the $t\bar{t}$ background. Four additional systematic uncertainties are considered for the $t\bar{t}$+$c\bar{c}$ background, derived from the simultaneous variation of factorisation and renormalisation scales, threshold of the parton-jet matching scheme [103], and c-quark mass variations in the simulation of $t\bar{t}$ events with Madgraph+Pythia, as well as the difference between simulations of the $t\bar{t}$+$c\bar{c}$ process with Madgraph+Pythia and Powheg+Pythia. For the $t\bar{t}$+$b\bar{b}$ background, eight additional systematic uncertainties are considered: three arise from scale uncertainties, one from the shower recoil model, two

JHEP03(2016)127

from the choice of PDF in the NLO prediction from Sherpa with OpenLoops and two from the uncertainties on multi-parton interaction and final-state radiation, which are not present in Sherpa with OpenLoops.

An uncertainty of $+5\%/-4\%$ is assumed for the cross section of single-top-quark production [56, 57], corresponding to the weighted average of the theoretical uncertainties on the s-, t- and Wt-channel production modes. One additional systematic uncertainty is considered to account for different ways of handling the interference between $t\bar{t}$ and Wt events [55]. For $t\bar{t}V$, an uncertainty of 30% on the cross section is assumed [52, 53] and an additional uncertainty arises from variations in the amount of radiation. The uncertainty on the $t\bar{t}H$ cross section is $+8.9\%/-12\%$ [11]. The uncertainties on the V+jets and diboson backgrounds are 48% and 25%, respectively [63, 68]. For events with 5 ($\geq$6 jets), one (two) additional uncertainties of 24% are added in quadrature to account for the extrapolation to higher jet multiplicities. In addition, the full difference between applying and not applying the p_{T} reweighting for the vector boson is taken as a systematic uncertainty. Uncertainties on the estimate of the multi-jet background come from the limited number of events in the data, especially at high jet and b-tagged jet multiplicities, from the uncertainties on the measured lepton misidentification rates (assumed to be 50%, but uncorrelated between events with an electron or muon), as well as from the subtraction of simulated events with a prompt lepton when estimating the misidentification rates.

Three sources of systematic uncertainty are considered when modelling $H^+ \to tb$ events. Uncertainties arising from the choice of PDF are estimated using samples generated with MC@NLO v4.6 [104] interfaced to Herwig++ v2.5.2 [105], by taking the envelope of the MSTW2008 68% CL NLO, CT10 NLO and NNPDF2.3 NLO PDF sets, and by normalising to the nominal cross section [101]. The uncertainties observed across the charged Higgs boson mass range are of the order of 5–10% and increase slightly with the H^+ mass. This systematic uncertainty affects both shape and normalisation. Uncertainties from the choice of the event generator are estimated from a comparison of the signal acceptances between events produced using either Powheg or Madgraph5_aMC@NLO v2.1.1 [106], both interfaced to Pythia v8.1, with a charged Higgs boson mass of 400 GeV. In the SR, this uncertainty is found to be about 1%, while it increases to as much as 20% in the CR. It is applied to all signal mass points as a normalisation-only systematic uncertainty. Uncertainties originating from initial- and final-state parton radiation, which can modify the jet production rate, are evaluated by varying factorisation/renormalisation scale parameters in the production of signal samples. This systematic uncertainty is found to be below 2% in all five event categories.

4.4 Results

A binned maximum likelihood fit to the data is performed simultaneously in the five event categories, and each mass hypothesis is tested separately. The inputs to the simultaneous fit are the distributions of $H_{\mathrm{T}}^{\mathrm{had}}$ in the four CR, and the BDT output histograms in the SR. The procedures for quantifying how well the data agree with the background-only hypothesis and for determining exclusion limits are based on the profile likelihood ratio test [107]. The parameter of interest is the production cross section $\sigma(gb \to tH^+)$ multiplied by the

JHEP03(2016)127

Source of uncertainty	Fractional uncertainty [%]	
	$m_{H^+} = 300\,\text{GeV}$	$m_{H^+} = 500\,\text{GeV}$
$t\bar{t}$ modelling	31	33
Jets	21	9.5
Flavour tagging	19	24
Other background modelling	9.6	12
Signal modelling	8.0	3.5
Lepton	1.2	0
Luminosity	1.1	0.4
Statistics	8.9	18

Table 3. Percentage of the total uncertainty on the signal strength that is induced from various systematic uncertainties. The values are obtained after fits to the background-plus-signal hypothesis. The largest contribution to the total uncertainty comes from the $t\bar{t}$ modelling.

branching fraction $\text{BR}(H^+ \to tb)$, also referred to as the signal strength. All systematic uncertainties, either from theoretical or experimental sources, are implemented as nuisance parameters with log-normal constraint terms. There are about 100 nuisance parameters considered in the fit, the number varying slightly across the range of mass hypotheses. The largest uncertainties for any tested mass point are those arising from the modelling of the $t\bar{t}$ processes. For $m_{H^+} < 350\,\text{GeV}$, the uncertainty on the $t\bar{t}$+$b\bar{b}$ cross section has the largest impact on the result. For higher mass hypotheses, the uncertainties on the shape of the distributions for $t\bar{t}$+$b\bar{b}$ from the reweighting to the NLO prediction are dominant. The fractional contributions of various sources of uncertainty to the total uncertainty on the parameter of interest are presented in table 3, for two hypothesised H^+ masses. The uncertainties decrease for higher mass hypotheses because of the larger signal acceptance and the improved separation between signal and background. The pulls of the nuisance parameters after profiling to the data are almost all within $\pm 1\sigma$ and never exceed $\pm 1.5\sigma$ for all tested mass hypotheses. The pulls that are larger than $\pm 1\sigma$ in at least one of the tested mass hypotheses are those associated with uncertainties on the $t\bar{t}$+HF cross sections, on the parton shower modelling of the $t\bar{t}$+$c\bar{c}$ process, and on the $t\bar{t}$+$b\bar{b}$ NLO modelling, derived from variations of the functional form of the renormalisation scale .

The post-fit distributions of the $H_{\text{T}}^{\text{had}}$ variable in the four CR for the fit under the background-only hypothesis are shown in figure 4, whereas the background-only post-fit distributions of the BDT output in the SR are presented in figure 5. The background component of a fit under the background-plus-signal hypothesis is overlayed. The post-fit event yields for the fit under the background-plus-signal hypothesis for $m_{H^+} = 300\,\text{GeV}$ are given in table 4. The fit prefers a positive signal strength for all tested mass hypotheses, except at 600 GeV. The post-fit event yields for the $t\bar{t}$+HF process are higher in background-only fits than those obtained in fits where the signal hypothesis is included.

The modified frequentist method (CLs) [108] and asymptotic formulae [109] are used to calculate upper limits on $\sigma(gb \to tH^+) \times \text{BR}(H^+ \to tb)$. The 95% confidence level (CL) upper limits are presented in figure 6. The mass hypotheses are tested in 25 GeV steps

JHEP03(2016)127

Process	4j(2b)	5j(2b)	≥6j(2b)	4j(≥3b)	≥5j(≥3b)
$t\bar{t}$+LF	83 600 ± 1900	41 800 ± 1400	21 000 ± 1000	6750 ± 270	6650 ± 390
$t\bar{t}$+$c\bar{c}$	3200 ± 1700	2600 ± 1400	2100 ± 1200	490 ± 230	1260 ± 570
$t\bar{t}$+$b\bar{b}$	1500 ± 530	1300 ± 440	1050 ± 450	600 ± 210	2040 ± 550
$t\bar{t}H$	34.6 ± 3.8	44.6 ± 4.9	66.7 ± 7.8	16.2 ± 1.9	87 ± 10
$t\bar{t}V$	132 ± 39	153 ± 46	186 ± 57	18.5 ± 5.4	87 ± 26
Single-top	5030 ± 530	1970 ± 270	860 ± 170	386 ± 55	342 ± 70
W+jets	4500 ± 1100	1660 ± 470	750 ± 270	250 ± 62	220 ± 69
Z+jets	1330 ± 560	370 ± 190	137 ± 80	56 ± 23	36 ± 27
VV	223 ± 63	103 ± 39	47 ± 23	10.4 ± 3.1	15.0 ± 5.3
Multi-jets	2230 ± 590	690 ± 180	330 ± 100	160 ± 46	208 ± 88
Total bkg	101 800 ± 2200	50 700 ± 1600	26 600 ± 1100	8730 ± 330	10 950 ± 490
H^+	700 ± 310	600 ± 260	430 ± 190	370 ± 160	990 ± 440
Data	102 462	51 421	26 948	9102	11 945

Table 4. Event yields of SM backgrounds, signal and data in all categories, after the fit to the data under the background-plus-signal hypothesis with a signal mass of 300 GeV. The last column shows the event yields in the SR. The uncertainties take into account correlations and constraints of the nuisance parameters.

between 200 and 300 GeV, and in 50 GeV steps up to 600 GeV. At 250 GeV, the local p_0-value for the observation to be in agreement with the background-only hypothesis reaches its smallest value of 0.9% (corresponding to 2.4 standard deviations). At m_{H^+} values of 300 and 450 GeV, the excess of the data with respect to the background-only hypothesis corresponds to 2.3 standard deviations.

For comparison, the expected upper limit is computed with a signal injected at $m_{H^+} = 300$ GeV, with a production cross section times branching fraction of 1.65 pb, corresponding to the best-fit value of the signal strength at this mass point. This results in an excess that is more localised at the injected mass value, i.e. extends less to lower and higher masses than the trend seen in the observed upper limit, as shown in figure 6. The H^+ signal is generated with a zero width. The experimental mass resolution ranges from approximately 30 GeV (for $m_{H^+} = 200$ GeV) up to 100 GeV (for $m_{H^+} = 600$ GeV) and is 50 GeV for the mass hypothesis of 300 GeV. A systematic background mismodelling is considerably more likely to give rise to the observed excess than a hypothesised signal at a specific mass. The cross sections of the $t\bar{t}$+HF backgrounds and the shape of the $t\bar{t}$+$b\bar{b}$ component have large uncertainties which are correlated with the signal normalisation. Together with the pre-fit excess of data compared to the SM prediction (table 1), this can result in a post-fit excess over a wide H^+ mass range. The fits were repeated using two alternative, less sensitive, discriminants in the SR: (a) a BDT trained against the sum of all backgrounds or (b) the variable $H_{\mathrm{T}}^{\mathrm{had}}$. Similar excesses were observed with these two alternative methods. The tested mass points are correlated with each other, since no mass-dependent event selections are applied in the analysis and the dataset is the same regardless of the hypothesised H^+ mass.

JHEP03(2016)127

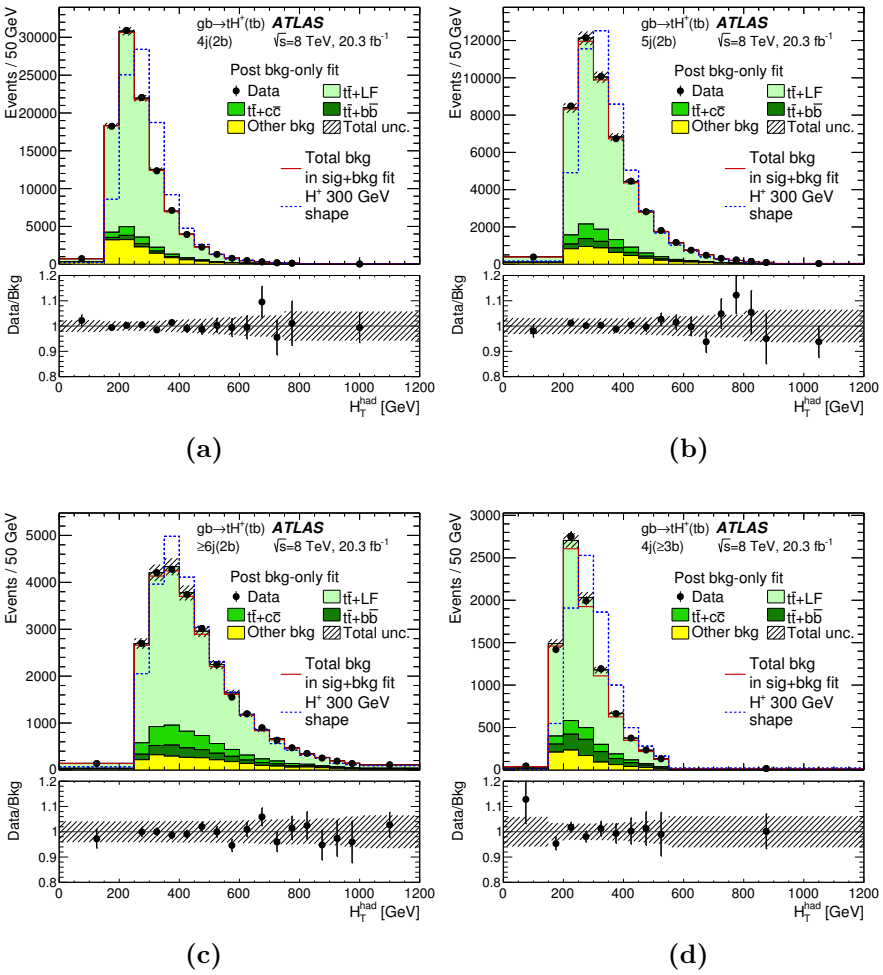

Figure 4. Distributions of $H_{\mathrm{T}}^{\mathrm{had}}$ after the fit to the data under the background-only hypothesis in the four control regions: (a) 4j(2b), (b) 5j(2b), (c) ≥6j(2b), (d) 4j(≥3b). Each background is normalised according to its post-fit cross section. The signal shape is shown as a superimposed dashed blue line normalised to the data. The last bin includes the overflow. The hatched bands show the post-fit uncertainties taking into account the constraints and correlations of the nuisance parameters. The lower panels display the ratio of the data to the total predicted background. In addition, the solid red line shows the total background after an unconditional fit under the background-plus-signal hypothesis with a signal mass of 300 GeV.

The limits in figure 6 are presented together with the signal prediction in the $m_h^{\mathrm{mod-}}$ benchmark scenario of the MSSM [95]. Model points with $0.5 \lesssim \tan\beta \lesssim 0.6$ and $\tan\beta \approx 0.5$ are excluded in the H^+ mass ranges of 200–300 GeV and 350–400 GeV, respectively,[4] while the expected limits in the mass range of 200–400 GeV reach $\tan\beta = 0.7$. The $m_h^{\mathrm{mod-}}$ scenario is chosen as a reference model, but similar exclusions are obtained in other relevant scenarios of the MSSM [95], i.e. $m_h^{\mathrm{mod+}}$, $m_h^{\mathrm{max-up}}$, *tau-phobic*, *light stau* and *light stop*. It has been verified that the width predicted by these models does not have a notable impact on the exclusions.

[4]No reliable theoretical predictions exist for $\tan\beta < 0.5$.

JHEP03(2016)127

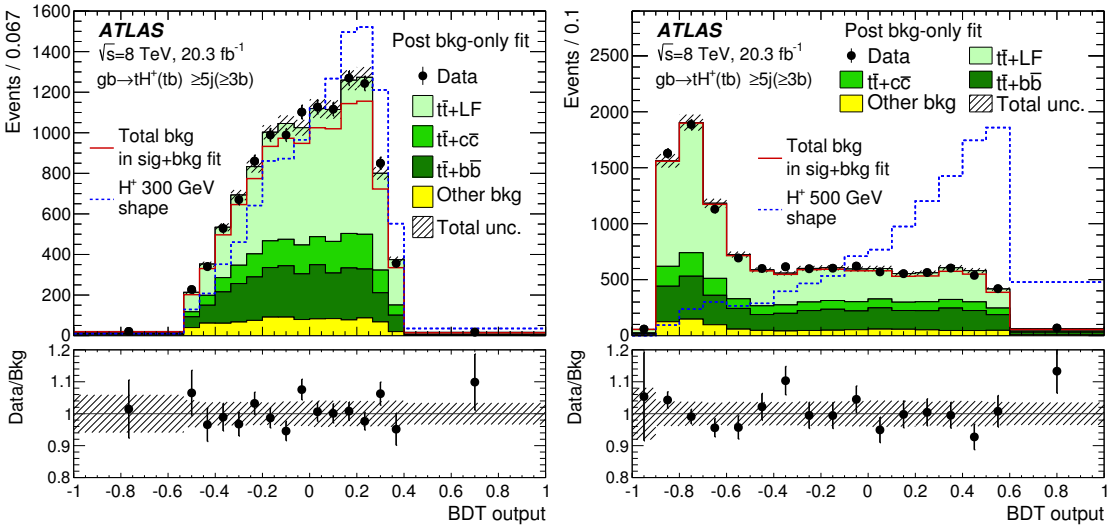

(a) (b)

Figure 5. Distributions of the BDT output in the signal-rich region after the fit to the data under the background-only hypothesis. The BDT was trained for two signal mass hypotheses: (a) 300 GeV and (b) 500 GeV. Each background is normalised according to its post-fit cross section. The signal shape is shown as a superimposed dashed blue line normalised to the data. The hatched bands show the post-fit uncertainties taking into account the constraints and correlations of the nuisance parameters. The lower panels display the ratio of the data to the total predicted background. In addition, the solid red line shows the total background after an unconditional fit under the background-plus-signal hypothesis with a signal mass of (a) 300 GeV and (b) 500 GeV.

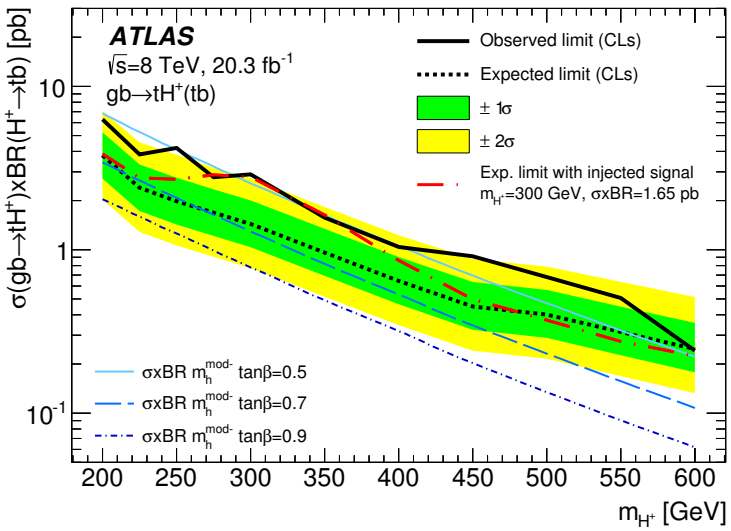

Figure 6. Expected and observed limits for the production of $H^+ \to tb$ in association with a top quark, as well as bands for 68% (in green) and 95% (in yellow) confidence intervals. The red dash-dotted line shows the expected limit obtained in the case where a simulated signal is injected at $m_{H^+} = 300$ GeV, with a production cross section times branching fraction of 1.65 pb (corresponding to the best-fit signal strength at that mass hypothesis), yielding a deviation from the expectation that extends less to higher and lower mass values than the observed upper limit. Theory predictions are shown for three representative values of $\tan\beta$ in the $m_h^{\mathrm{mod}-}$ benchmark scenario of the MSSM.

JHEP03(2016)127

5 Search for a charged Higgs boson produced in the s-channel

In this section, two searches for $qq' \to W' \to tb$ recently published by ATLAS [22, 23] are reinterpreted as searches for the s-channel production[5] of charged Higgs bosons, i.e. $qq' \to H^+ \to tb$, based on final states with one charged lepton (electron or muon) and jets, or hadronic jets only.

5.1 Lepton+jets final state

In the search for $H^+ \to tb \to (\ell\nu b)b$ produced in the s-channel, where the charged lepton ℓ is an electron or muon (from a prompt W-boson decay or a leptonic τ decay), only events collected using a single-electron or single-muon trigger are considered, with the same combination of thresholds as in section 4.1. Exactly one charged lepton is required, which must match, with $\Delta R < 0.15$, a lepton reconstructed by the trigger. The electron or muon is then required to have E_{T} or p_{T} greater than 30 GeV. The selected events must then have two or three jets, with exactly two of them b-tagged. In addition, the $E_{\mathrm{T}}^{\mathrm{miss}}$ must exceed 35 GeV, and the sum $E_{\mathrm{T}}^{\mathrm{miss}} + m_{\mathrm{T}}$, where m_{T} is the transverse mass[6] of the W boson, is required to be greater than 60 GeV in order to reduce the contribution from the multi-jet background. Assuming that the missing transverse momentum arises solely from the neutrino in the W-boson decay, its transverse momentum is given by the x- and y-components of the $E_{\mathrm{T}}^{\mathrm{miss}}$ vector, while the unmeasured z-component of the neutrino momentum p_z^ν is inferred by imposing the W-boson mass constraint on the lepton-neutrino system. This leads to a quadratic equation for p_z^ν. In the case of two real solutions, the one with the smaller p_z^ν is chosen. If the solutions are complex, a real estimate of the p_z^ν is obtained by a kinematic fit that rescales the neutrino momentum components p_x^ν and p_y^ν such that the imaginary term vanishes. The corrected missing transverse momentum of the neutrino is kept as close as possible to the measured $E_{\mathrm{T}}^{\mathrm{miss}}$ [110].

Having determined the four-momentum of the leptonically decaying W boson, the top quark is then reconstructed. The b-tagged jet for which the invariant mass of the Wb system is closest to m_{top} is assumed to originate from the top-quark decay, the other b-tagged jet being in turn assigned to the H^+ decay. The selected events are then classified into one signal-rich and one signal-depleted region, separately for events with two or three jets. The signal-rich region is the subset of the sample with two b-tagged jets and an invariant mass $m_{tb} > 330$ GeV. The signal-depleted region is the complementary subset, with two b-tagged jets and $m_{tb} < 330$ GeV.

The shape and normalisation of the multi-jet background with a misidentified lepton are determined with the matrix method [31]. All other backgrounds are taken from simulation. For W+jets events, the sample composition in the signal-rich and signal-depleted regions with two b-tagged jets are similar, hence an overall renormalisation of the W+jets background, based on the event yield measured in the signal-depleted region, is applied to the events with two jets. In the events with three jets, the contribution of the W+jets

[5] While the process generated is $qq' \to H^+$, the most commonly occuring reaction is $cs \to H^+$.

[6] The transverse mass is defined as $m_{\mathrm{T}} = \sqrt{2p_{\mathrm{T}}^{\ell} E_{\mathrm{T}}^{\mathrm{miss}} (1 - \cos\Delta\phi_{\ell,\mathrm{miss}})}$, where $\Delta\phi_{\ell,\mathrm{miss}}$ is the azimuthal separation between the reconstructed lepton and the missing momentum in the transverse plane.

JHEP03(2016)127

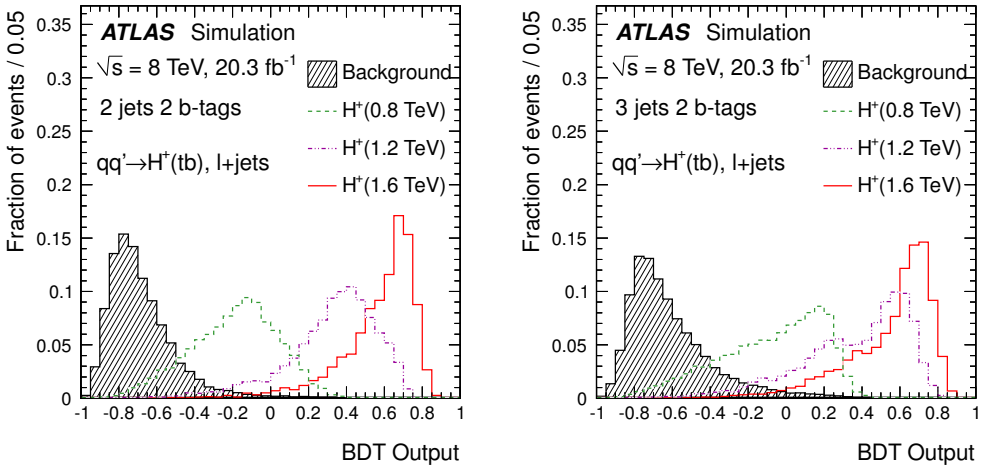

(a) **(b)**

Figure 7. Expected BDT output distribution for the SM backgrounds and for three H^+ signal samples (with masses of 0.8, 1.2 and 1.6 TeV), obtained in the signal-rich regions with (a) 2 jets and 2 b-tags and (b) 3 jets and 2 b-tags. All distributions are averaged over events with an electron or a muon in the final state, and they are normalised to unity.

background remains below 10% and large uncertainties are obtained for the data-driven renormalisation factors, hence the W+jets process with three jets is treated in the same way as the other simulated backgrounds.

BDT discriminators, using the TMVA toolkit [99], are again used to obtain the best separation between the $H^+ \to tb$ signal events and the associated SM backgrounds. The same BDT as in the search for $W' \to tb$ [22] are used. These BDT were trained for a W' mass of 1.75 TeV. Alternative trainings with H^+ samples were tested but no overall improvement of the expected sensitivity was found. In events with two (three) jets, ten (eleven) BDT input variables are used, of which m_{tb} and the p_{T} of the top-quark candidate are the most discriminating. Figure 7 shows the expected BDT output distributions, normalised to unity, for selected $H^+ \to tb$ signal samples and the background processes, in the signal-rich regions.

No sign of a signal is observed in the selected samples with two or three jets, including two b-tags [22], as illustrated in figure 8. The BDT distributions of events with 2-jet and 3-jet final states, with separated e+jets and μ+jets samples, are used in a combined statistical analysis to compute exclusion limits on the cross section times branching fraction for $H^+ \to tb$ in the s-channel production mode, as discussed in section 5.3.

5.2 All-hadronic final state

In this section, the search for $H^+ \to tb \to (qq'b)b$ produced in the s-channel is described. The selection and the statistical analysis are identical to those of the $W' \to tb$ search [23]. Events with isolated charged leptons are vetoed in the event selection. Candidate events are first collected using the requirement that the scalar sum of E_{T} for all energy deposits

JHEP03(2016)127

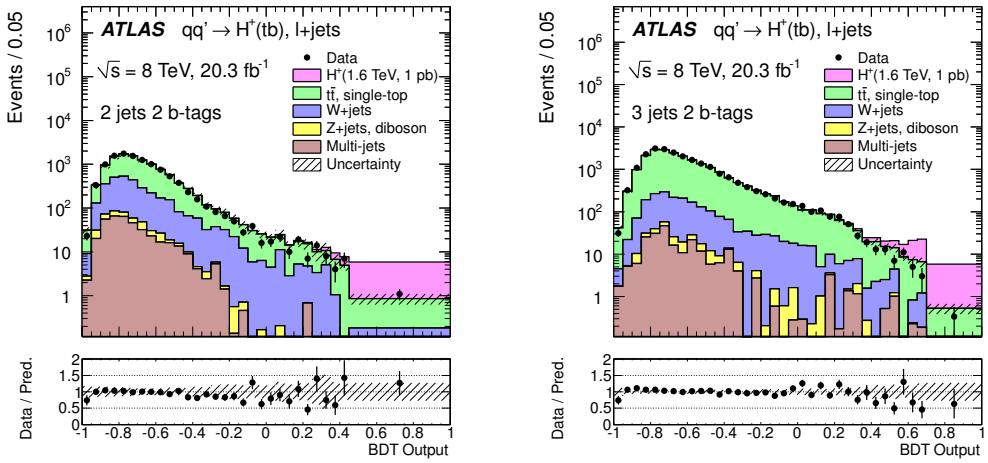

(a) **(b)**

Figure 8. Comparison of the BDT output distributions between the ATLAS data and simulation, in the signal-rich regions with (a) 2 jets and 2 b-tags and (b) 3 jets and 2 b-tags, summing the events with an electron or a muon in the final state. A potential signal contribution, with a charged Higgs boson mass of 1.6 TeV and a cross section times branching fraction of 1 pb, is shown stacked on top of the background distributions. The uncertainty bands include normalisation uncertainties on all backgrounds and the uncertainty due to the limited size of the samples of simulated events.

in the calorimeters exceeds 700 GeV at the trigger level. Then, the scalar sum of p_{T} of all small-radius jets is required to be greater than 850 GeV. The selected events must contain exactly one top-tagged large-radius jet (reconstructed and identified using the procedure described in section 3) with $p_{\mathrm{T}} > 350$ GeV and $|\eta| < 2.0$. A small-radius b-tagged jet, with $p_{\mathrm{T}} > 350$ GeV and a separation $\Delta R > 2.0$ from the top-tagged jet, is also required. The invariant mass of the top-tagged jet and the b-tagged jet, m_{tb}, must exceed 1.1 TeV. The selected events are classified into two categories, one b-tag or two b-tags, depending on whether or not an additional small-radius b-tagged jet with $p_{\mathrm{T}} > 25$ GeV is found with a distance $\Delta R < 1.0$ from the top-tagged jet. The second b-tagged jet, if found, is used for classification only and does not enter the invariant mass calculation, to avoid double-counting of energy.

The shape of the m_{tb} distribution for the signal is estimated from a fit to simulated H^+ events. The appropriate functional form is found to be the same as in the search for $W' \to tb$: a skew-normal distribution convolved with a Gaussian function, to capture the asymmetric structure of the H^+ signal shape due to radiation, together with off-shell production [23]. The signal shapes are shown in figure 9.

A fit of the SM background plus the H^+ signal shape to the data is used to estimate the background. The background shape is described by an exponential function with a polynomial of order n as argument, $\exp(\sum_{k=1}^{n} c_k m_{tb}^k)$ with $n = 4\,(2)$ in the one (two) b-tag category. The function was selected to optimally describe the SM background as estimated from fits to signal-free control regions, as well as to minimise the number of spurious signal events found in the background-plus-signal fit to this background-only sample. Multi-jet

JHEP03(2016)127

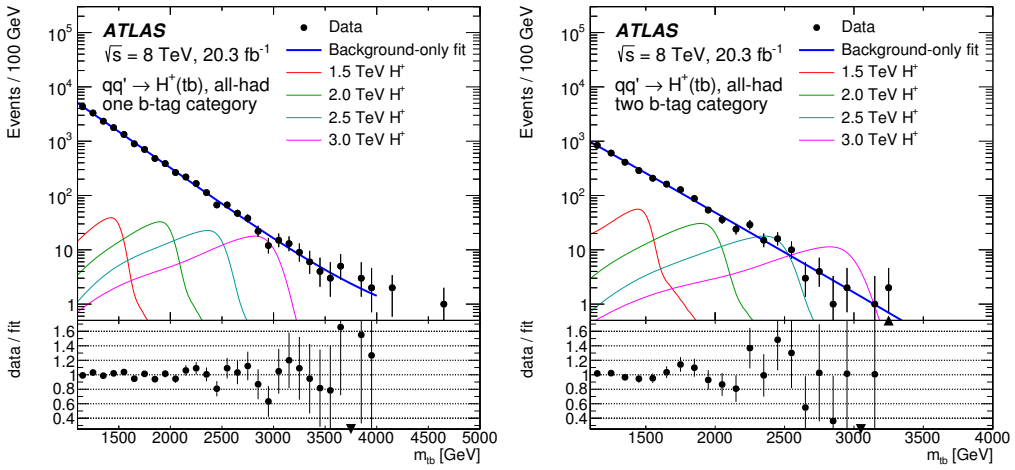

Figure 9. The m_{tb} distribution in data, with a background-only fit, in the (a) one b-tag and (b) two b-tag categories. The lower panels show the ratio of the data to the fit. Potential signal contributions, with charged Higgs boson masses of 1.5, 2.0, 2.5 and 3.0 TeV, each corresponding to a cross section times branching fraction of 0.2 pb, are also shown.

events contribute at the level of 99% (88%) to the total background in the one (two) b-tag event categories, as estimated from simulation and fits to the data in control regions [23].

No significant excess of data with respect to the SM predictions is observed in the selected samples with one or two b-tags, as shown in the search for $W' \to tb$ [23] and illustrated in figure 9. The m_{tb} distributions in the one and two b-tag event categories are used in a combined statistical analysis to compute exclusion limits, as discussed in section 5.3.

5.3 Results and interpretations

The data are found to be compatible with the background-only predictions [22, 23], and 95% CL upper limits on the production cross section times branching fraction of $H^+ \to tb$ in the s-channel are derived using a narrow-width approximation. Hypothesis testing is performed using the CLs [108] procedure, with the log-likelihood ratio of the background-plus-signal and background-only hypotheses as the test statistic for both final states. Systematic uncertainties are treated as nuisance parameters and are implemented in the same manner as in the searches for $W' \to tb$ [22, 23], with the exception of the uncertainty arising from the choice of the PDF in the signal modelling, since the colliding partons are mainly c- and s-quarks in the H^+ production. The PDF systematic uncertainties are estimated by taking the envelope of the MSTW2008 68% CL NLO, CT10 NLO and NNPDF3.0 NLO PDF sets in nominal H^+ signal events, reweighted using LHAPDF6 [111]. The dominant systematic uncertainty in the lepton+jets final state is the W+jets cross section normalisation, while for the all-hadronic final state, the b-tagging and background modelling uncertainties dominate. Figure 10 shows the expected and observed 95% CL upper limits on the production cross section times branching fraction of $qq' \to H^+ \to tb$ in the s-channel. For the lep-

JHEP03(2016)127

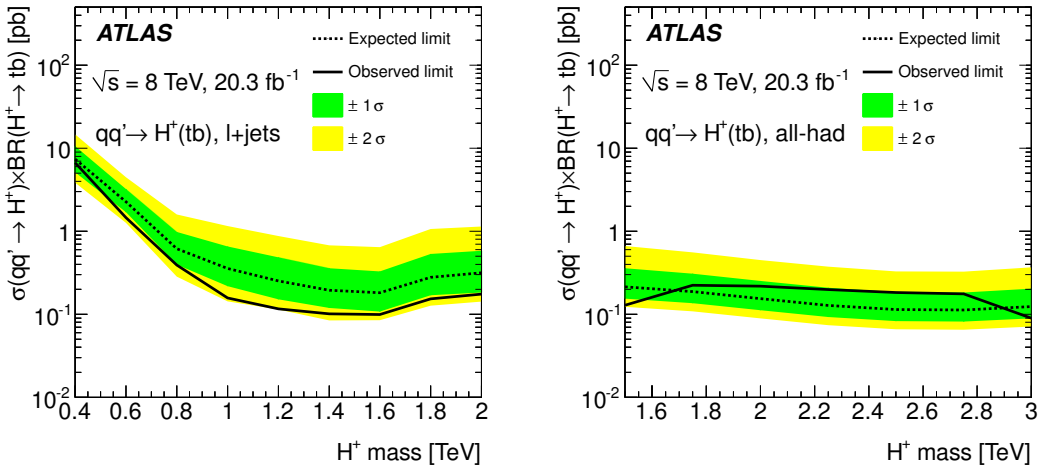

(a) **(b)**

Figure 10. Expected and observed 95% CL limits on the s-channel production cross section times branching fraction for $H^+ \to tb$ as a function of the charged Higgs boson mass, in the (a) lepton+jets final state and (b) all-hadronic final state, including all systematic uncertainties, using a narrow-width approximation.

ton+jets (all-hadronic) final state and the charged Higgs boson mass range of 0.4–2.0 TeV (1.5–3.0 TeV), these observed upper limits lie between 0.13 and 6.7 pb (0.09 and 0.22 pb). The corresponding expected upper limits on the cross section times branching fraction are 0.18–7.4 pb (0.11–0.21 pb). These limits are valid for a narrow-width approximation, i.e. when the decay width divided by the mass is small ($\Gamma(H^+ \to tb)/m_{H^+} < 1.5\%$) compared with the detector resolution (∼10%).

No exclusion of a type-II 2HDM in a narrow-width approximation can be made based on the observed limits. However, these generic upper limits are the first ones from ATLAS for a narrow charged scalar particle produced through annihilation of light quarks and decaying into a tb pair. This could enable the probing of charged Higgs bosons (other than type-II 2HDM) that also have sizeable couplings to lighter quarks.

6 Conclusions

This paper presents searches for charged Higgs bosons decaying through $H^+ \to tb$, produced either in association with a top quark or in the s-channel process $qq' \to H^+ \to tb$, using the 20.3 fb^{-1} dataset of pp collisions at $\sqrt{s} = 8$ TeV collected by the ATLAS experiment at the LHC during Run 1.

The search for $gb \to tH^+$ is performed in the H^+ mass range of 200–600 GeV. The analysis uses multivariate analysis techniques in the signal-rich region, and it employs control regions to reduce the large uncertainties on the backgrounds. An excess of data with respect to the SM predictions is observed for all H^+ mass hypotheses, except 600 GeV. The injection of simulated H^+ events yields a deviation from the expectation that extends less to higher and lower masses than the observed upper limit, indicating that a systematic

JHEP03(2016)127

background mismodelling is more likely to give rise to the observed excess than a signal. The smallest local p_0-values are found at m_{H^+} values of 250, 300 and 450 GeV, corresponding to 2.3–2.4 standard deviations. The $m_h^{\text{mod}-}$ scenario of the Minimal Supersymmetric Standard Model is excluded at 95% confidence level for $0.5 \lesssim \tan\beta \lesssim 0.6$ in the H^+ mass range of 200–300 GeV, and for $\tan\beta \approx 0.5$ in the H^+ mass range of 350–400 GeV.

The s-channel production of $qq' \to H^+ \to tb$ is investigated through a reinterpretation of searches for $W' \to tb$ in ATLAS. The lepton+jets final state is used for H^+ masses between 0.4 and 2.0 TeV, and the search employs multivariate techniques in order to reduce the contribution of SM backgrounds. The all-hadronic final state is used in the H^+ mass range of 1.5–3.0 TeV, and events with a jet tagged as originating from a hadronic top-quark decay are selected in the analysis. In both searches for $H^+ \to tb$ produced via the s-channel process, no significant excess of data is observed with respect to the SM predictions. The s-channel production mode offers a possibility to probe the coupling between light quarks and a charged Higgs boson. No upper limits on the cross section of charged scalar particles in the s-channel production mode have been set previously by the ATLAS experiment.

Acknowledgments

We thank CERN for the very successful operation of the LHC, as well as the support staff from our institutions without whom ATLAS could not be operated efficiently.

We acknowledge the support of ANPCyT, Argentina; YerPhI, Armenia; ARC, Australia; BMWFW and FWF, Austria; ANAS, Azerbaijan; SSTC, Belarus; CNPq and FAPESP, Brazil; NSERC, NRC and CFI, Canada; CERN; CONICYT, Chile; CAS, MOST and NSFC, China; COLCIENCIAS, Colombia; MSMT CR, MPO CR and VSC CR, Czech Republic; DNRF, DNSRC and Lundbeck Foundation, Denmark; IN2P3-CNRS, CEA-DSM/IRFU, France; GNSF, Georgia; BMBF, HGF, and MPG, Germany; GSRT, Greece; RGC, Hong Kong SAR, China; ISF, I-CORE and Benoziyo Center, Israel; INFN, Italy; MEXT and JSPS, Japan; CNRST, Morocco; FOM and NWO, Netherlands; RCN, Norway; MNiSW and NCN, Poland; FCT, Portugal; MNE/IFA, Romania; MES of Russia and NRC KI, Russian Federation; JINR; MESTD, Serbia; MSSR, Slovakia; ARRS and MIZŠ, Slovenia; DST/NRF, South Africa; MINECO, Spain; SRC and Wallenberg Foundation, Sweden; SERI, SNSF and Cantons of Bern and Geneva, Switzerland; MOST, Taiwan; TAEK, Turkey; STFC, United Kingdom; DOE and NSF, United States of America. In addition, individual groups and members have received support from BCKDF, the Canada Council, CANARIE, CRC, Compute Canada, FQRNT, and the Ontario Innovation Trust, Canada; EPLANET, ERC, FP7, Horizon 2020 and Marie Skłodowska-Curie Actions, European Union; Investissements d'Avenir Labex and Idex, ANR, Region Auvergne and Fondation Partager le Savoir, France; DFG and AvH Foundation, Germany; Herakleitos, Thales and Aristeia programmes co-financed by EU-ESF and the Greek NSRF; BSF, GIF and Minerva, Israel; BRF, Norway; the Royal Society and Leverhulme Trust, United Kingdom.

The crucial computing support from all WLCG partners is acknowledged gratefully, in particular from CERN and the ATLAS Tier-1 facilities at TRIUMF (Canada), NDGF (Denmark, Norway, Sweden), CC-IN2P3 (France), KIT/GridKA (Germany), INFN-CNAF (Italy), NL-T1 (Netherlands), PIC (Spain), ASGC (Taiwan), RAL (U.K.) and BNL (U.S.A.) and in the Tier-2 facilities worldwide.

JHEP03(2016)127

References

[1] ATLAS collaboration, *Observation of a new particle in the search for the Standard Model Higgs boson with the ATLAS detector at the LHC*, *Phys. Lett.* **B 716** (2012) 1 [arXiv:1207.7214] [INSPIRE].

[2] CMS collaboration, *Observation of a new boson at a mass of* 125 *GeV with the CMS experiment at the LHC*, *Phys. Lett.* **B 716** (2012) 30 [arXiv:1207.7235] [INSPIRE].

[3] ATLAS, CMS collaborations, *Combined Measurement of the Higgs Boson Mass in pp Collisions at* $\sqrt{s} = 7$ *and* 8 *TeV with the ATLAS and CMS Experiments*, *Phys. Rev. Lett.* **114** (2015) 191803 [arXiv:1503.07589] [INSPIRE].

[4] T.D. Lee, *A Theory of Spontaneous T Violation*, *Phys. Rev.* **D 8** (1973) 1226 [INSPIRE].

[5] T.P. Cheng and L.-F. Li, *Neutrino Masses, Mixings and Oscillations in* SU(2) × U(1) *Models of Electroweak Interactions*, *Phys. Rev.* **D 22** (1980) 2860 [INSPIRE].

[6] J. Schechter and J.W.F. Valle, *Neutrino Masses in* SU(2) × U(1) *Theories*, *Phys. Rev.* **D 22** (1980) 2227 [INSPIRE].

[7] G. Lazarides, Q. Shafi and C. Wetterich, *Proton Lifetime and Fermion Masses in an* SO(10) *Model*, *Nucl. Phys.* **B 181** (1981) 287 [INSPIRE].

[8] R.N. Mohapatra and G. Senjanović, *Neutrino Masses and Mixings in Gauge Models with Spontaneous Parity Violation*, *Phys. Rev.* **D 23** (1981) 165 [INSPIRE].

[9] M. Magg and C. Wetterich, *Neutrino Mass Problem and Gauge Hierarchy*, *Phys. Lett.* **B 94** (1980) 61 [INSPIRE].

[10] R. Harlander, M. Krämer and M. Schumacher, *Bottom-quark associated Higgs-boson production: reconciling the four- and five-flavour scheme approach*, arXiv:1112.3478 [INSPIRE].

[11] LHC Higgs Cross Section Working Group, J.R. Andersen et al., *Handbook of LHC Higgs Cross Sections: 3. Higgs Properties*, CERN-2013-004 [arXiv:1307.1347] [INSPIRE].

[12] LEP, DELPHI, OPAL, ALEPH, L3 collaborations, G. Abbiendi et al., *Search for Charged Higgs bosons: Combined Results Using LEP Data*, *Eur. Phys. J.* **C 73** (2013) 2463 [arXiv:1301.6065] [INSPIRE].

[13] CDF collaboration, T. Aaltonen et al., *Search for charged Higgs bosons in decays of top quarks in* $p\bar{p}$ *collisions at* $\sqrt{s} = 1.96$ *TeV*, *Phys. Rev. Lett.* **103** (2009) 101803 [arXiv:0907.1269] [INSPIRE].

[14] D0 collaboration, V.M. Abazov et al., *Search for Charged Higgs Bosons in Top Quark Decays*, *Phys. Lett.* **B 682** (2009) 278 [arXiv:0908.1811] [INSPIRE].

[15] D0 collaboration, V.M. Abazov et al., *Search for charged Higgs bosons decaying to top and bottom quarks in* $p\bar{p}$ *collisions*, *Phys. Rev. Lett.* **102** (2009) 191802 [arXiv:0807.0859] [INSPIRE].

[16] CMS collaboration, *Search for a light charged Higgs boson in top quark decays in pp collisions at* $\sqrt{s} = 7$ *TeV*, *JHEP* **07** (2012) 143 [arXiv:1205.5736] [INSPIRE].

JHEP03(2016)127

[17] ATLAS collaboration, *Search for charged Higgs bosons decaying via $H^+ \to \tau\nu$ in top quark pair events using pp collision data at $\sqrt{s} = 7$ TeV with the ATLAS detector*, *JHEP* **06** (2012) 039 [arXiv:1204.2760] [INSPIRE].

[18] ATLAS collaboration, *Search for charged Higgs bosons through the violation of lepton universality in $t\bar{t}$ events using pp collision data at $\sqrt{s} = 7$ TeV with the ATLAS experiment*, *JHEP* **03** (2013) 076 [arXiv:1212.3572] [INSPIRE].

[19] ATLAS collaboration, *Search for charged Higgs bosons decaying via $H^\pm \to \tau^\pm\nu$ in fully hadronic final states using pp collision data at $\sqrt{s} = 8$ TeV with the ATLAS detector*, *JHEP* **03** (2015) 088 [arXiv:1412.6663] [INSPIRE].

[20] CMS collaboration, *Search for a charged Higgs boson in pp collisions at $\sqrt{s} = 8$ TeV*, *JHEP* **11** (2015) 018 [arXiv:1508.07774] [INSPIRE].

[21] ATLAS collaboration, *Search for a Charged Higgs Boson Produced in the Vector-Boson Fusion Mode with Decay $H^\pm \to W^\pm Z$ using pp Collisions at $\sqrt{s} = 8$ TeV with the ATLAS Experiment*, *Phys. Rev. Lett.* **114** (2015) 231801 [arXiv:1503.04233] [INSPIRE].

[22] ATLAS collaboration, *Search for $W' \to t\bar{b}$ in the lepton plus jets final state in proton-proton collisions at a centre-of-mass energy of $\sqrt{s} = 8$ TeV with the ATLAS detector*, *Phys. Lett.* **B 743** (2015) 235 [arXiv:1410.4103] [INSPIRE].

[23] ATLAS collaboration, *Search for $W' \to tb \to qqbb$ decays in pp collisions at $\sqrt{s} = 8$ TeV with the ATLAS detector*, *Eur. Phys. J.* **C 75** (2015) 165 [arXiv:1408.0886] [INSPIRE].

[24] P. Fayet, *Supersymmetry and Weak, Electromagnetic and Strong Interactions*, *Phys. Lett.* **B 64** (1976) 159 [INSPIRE].

[25] P. Fayet, *Spontaneously Broken Supersymmetric Theories of Weak, Electromagnetic and Strong Interactions*, *Phys. Lett.* **B 69** (1977) 489 [INSPIRE].

[26] G.R. Farrar and P. Fayet, *Phenomenology of the Production, Decay and Detection of New Hadronic States Associated with Supersymmetry*, *Phys. Lett.* **B 76** (1978) 575 [INSPIRE].

[27] P. Fayet, *Relations Between the Masses of the Superpartners of Leptons and Quarks, the Goldstino Couplings and the Neutral Currents*, *Phys. Lett.* **B 84** (1979) 416 [INSPIRE].

[28] S. Dimopoulos and H. Georgi, *Softly Broken Supersymmetry and* SU(5), *Nucl. Phys.* **B 193** (1981) 150 [INSPIRE].

[29] ATLAS collaboration, *The ATLAS Experiment at the CERN Large Hadron Collider*, 2008 *JINST* **3** S08003 [INSPIRE].

[30] ATLAS collaboration, *Improved luminosity determination in pp collisions at $\sqrt{s} = 7$ TeV using the ATLAS detector at the LHC*, *Eur. Phys. J.* **C 73** (2013) 2518 [arXiv:1302.4393] [INSPIRE].

[31] ATLAS collaboration, *Estimation of non-prompt and fake lepton backgrounds in final states with top quarks produced in proton-proton collisions at $\sqrt{s} = 8$ TeV with the ATLAS detector*, ATLAS-CONF-2014-058.

[32] S. Frixione, P. Nason and G. Ridolfi, *A Positive-weight next-to-leading-order Monte Carlo for heavy flavour hadroproduction*, *JHEP* **09** (2007) 126 [arXiv:0707.3088] [INSPIRE].

[33] S. Alioli, P. Nason, C. Oleari and E. Re, *A general framework for implementing NLO calculations in shower Monte Carlo programs: the POWHEG BOX*, *JHEP* **06** (2010) 043 [arXiv:1002.2581] [INSPIRE].

JHEP03(2016)127

[34] H.-L. Lai et al., *New parton distributions for collider physics*, *Phys. Rev.* **D 82** (2010) 074024 [arXiv:1007.2241] [INSPIRE].

[35] J. Gao et al., *CT10 next-to-next-to-leading order global analysis of QCD*, *Phys. Rev.* **D 89** (2014) 033009 [arXiv:1302.6246] [INSPIRE].

[36] T. Sjöstrand et al., *High-energy physics event generation with PYTHIA 6.1*, *Comput. Phys. Commun.* **135** (2001) 238 [hep-ph/0010017] [INSPIRE].

[37] P.Z. Skands, *Tuning Monte Carlo Generators: The Perugia Tunes*, *Phys. Rev.* **D 82** (2010) 074018 [arXiv:1005.3457] [INSPIRE].

[38] M. Cacciari, M. Czakon, M. Mangano, A. Mitov and P. Nason, *Top-pair production at hadron colliders with next-to-next-to-leading logarithmic soft-gluon resummation*, *Phys. Lett.* **B 710** (2012) 612 [arXiv:1111.5869] [INSPIRE].

[39] M. Beneke, P. Falgari, S. Klein and C. Schwinn, *Hadronic top-quark pair production with NNLL threshold resummation*, *Nucl. Phys.* **B 855** (2012) 695 [arXiv:1109.1536] [INSPIRE].

[40] P. Bärnreuther, M. Czakon and A. Mitov, *Percent Level Precision Physics at the Tevatron: First Genuine NNLO QCD Corrections to $q\bar{q} \to t\bar{t} + X$*, *Phys. Rev. Lett.* **109** (2012) 132001 [arXiv:1204.5201] [INSPIRE].

[41] M. Czakon and A. Mitov, *NNLO corrections to top-pair production at hadron colliders: the all-fermionic scattering channels*, *JHEP* **12** (2012) 054 [arXiv:1207.0236] [INSPIRE].

[42] M. Czakon and A. Mitov, *NNLO corrections to top pair production at hadron colliders: the quark-gluon reaction*, *JHEP* **01** (2013) 080 [arXiv:1210.6832] [INSPIRE].

[43] M. Czakon, P. Fiedler and A. Mitov, *Total Top-Quark Pair-Production Cross Section at Hadron Colliders Through $O(\alpha_S^4)$*, *Phys. Rev. Lett.* **110** (2013) 252004 [arXiv:1303.6254] [INSPIRE].

[44] M. Czakon and A. Mitov, *Top++: A Program for the Calculation of the Top-Pair Cross-Section at Hadron Colliders*, *Comput. Phys. Commun.* **185** (2014) 2930 [arXiv:1112.5675] [INSPIRE].

[45] ATLAS collaboration, *Search for the Standard Model Higgs boson produced in association with top quarks and decaying into $b\bar{b}$ in pp collisions at $\sqrt{s} = 8$ TeV with the ATLAS detector*, *Eur. Phys. J.* **C 75** (2015) 349 [arXiv:1503.05066] [INSPIRE].

[46] ATLAS collaboration, *Measurements of normalized differential cross sections for $t\bar{t}$ production in pp collisions at $\sqrt{s} = 7$ TeV using the ATLAS detector*, *Phys. Rev.* **D 90** (2014) 072004 [arXiv:1407.0371] [INSPIRE].

[47] T. Gleisberg et al., *Event generation with SHERPA 1.1*, *JHEP* **02** (2009) 007 [arXiv:0811.4622] [INSPIRE].

[48] F. Cascioli, P. Maierhofer and S. Pozzorini, *Scattering Amplitudes with Open Loops*, *Phys. Rev. Lett.* **108** (2012) 111601 [arXiv:1111.5206] [INSPIRE].

[49] J. Alwall, M. Herquet, F. Maltoni, O. Mattelaer and T. Stelzer, *MadGraph 5: Going Beyond*, *JHEP* **06** (2011) 128 [arXiv:1106.0522] [INSPIRE].

[50] P.M. Nadolsky et al., *Implications of CTEQ global analysis for collider observables*, *Phys. Rev.* **D 78** (2008) 013004 [arXiv:0802.0007] [INSPIRE].

[51] ATLAS collaboration, *ATLAS tunes of PYTHIA 6 and PYTHIA 8 for MC11*, ATL-PHYS-PUB-2011-009 (2011).

JHEP03(2016)127

[52] J.M. Campbell and R.K. Ellis, *$t\bar{t}W^{\pm}$ production and decay at NLO*, *JHEP* **07** (2012) 052 [arXiv:1204.5678] [INSPIRE].

[53] M.V. Garzelli, A. Kardos, C.G. Papadopoulos and Z. Trócsányi, *$t\,\bar{t}\,W^{\pm}$ and $t\,\bar{t}\,Z$ Hadroproduction at NLO accuracy in QCD with Parton Shower and Hadronization effects*, *JHEP* **11** (2012) 056 [arXiv:1208.2665] [INSPIRE].

[54] B.P. Kersevan and E. Richter-Was, *The Monte Carlo event generator AcerMC versions 2.0 to 3.8 with interfaces to PYTHIA 6.4, HERWIG 6.5 and ARIADNE 4.1*, *Comput. Phys. Commun.* **184** (2013) 919 [hep-ph/0405247] [INSPIRE].

[55] S. Frixione, E. Laenen, P. Motylinski, B.R. Webber and C.D. White, *Single-top hadroproduction in association with a W boson*, *JHEP* **07** (2008) 029 [arXiv:0805.3067] [INSPIRE].

[56] N. Kidonakis, *Next-to-next-to-leading-order collinear and soft gluon corrections for t-channel single top quark production*, *Phys. Rev.* **D 83** (2011) 091503 [arXiv:1103.2792] [INSPIRE].

[57] N. Kidonakis, *NNLL resummation for s-channel single top quark production*, *Phys. Rev.* **D 81** (2010) 054028 [arXiv:1001.5034] [INSPIRE].

[58] N. Kidonakis, *Two-loop soft anomalous dimensions for single top quark associated production with a W^- or H^-*, *Phys. Rev.* **D 82** (2010) 054018 [arXiv:1005.4451] [INSPIRE].

[59] A.D. Martin, W.J. Stirling, R.S. Thorne and G. Watt, *Parton distributions for the LHC*, *Eur. Phys. J.* **C 63** (2009) 189 [arXiv:0901.0002] [INSPIRE].

[60] A.D. Martin, W.J. Stirling, R.S. Thorne and G. Watt, *Uncertainties on α_S in global PDF analyses and implications for predicted hadronic cross sections*, *Eur. Phys. J.* **C 64** (2009) 653 [arXiv:0905.3531] [INSPIRE].

[61] A.D. Martin, W.J. Stirling, R.S. Thorne and G. Watt, *Heavy-quark mass dependence in global PDF analyses and 3- and 4-flavour parton distributions*, *Eur. Phys. J.* **C 70** (2010) 51 [arXiv:1007.2624] [INSPIRE].

[62] M.L. Mangano, M. Moretti, F. Piccinini, R. Pittau and A.D. Polosa, *ALPGEN, a generator for hard multiparton processes in hadronic collisions*, *JHEP* **07** (2003) 001 [hep-ph/0206293] [INSPIRE].

[63] K. Melnikov and F. Petriello, *Electroweak gauge boson production at hadron colliders through $O(\alpha_S^2)$*, *Phys. Rev.* **D 74** (2006) 114017 [hep-ph/0609070] [INSPIRE].

[64] ATLAS collaboration, *Measurement of the production cross section of jets in association with a Z boson in pp collisions at $\sqrt{s} = 7$ TeV with the ATLAS detector*, *JHEP* **07** (2013) 032 [arXiv:1304.7098] [INSPIRE].

[65] G. Corcella et al., *HERWIG 6: An Event generator for hadron emission reactions with interfering gluons (including supersymmetric processes)*, *JHEP* **01** (2001) 010 [hep-ph/0011363] [INSPIRE].

[66] J.M. Butterworth, J.R. Forshaw and M.H. Seymour, *Multiparton interactions in photoproduction at HERA*, *Z. Phys.* **C 72** (1996) 637 [hep-ph/9601371] [INSPIRE].

[67] ATLAS collaboration, *New ATLAS event generator tunes to 2010 data*, ATL-PHYS-PUB-2011-008 (2011).

[68] J.M. Campbell and R.K. Ellis, *MCFM for the Tevatron and the LHC*, *Nucl. Phys. Proc. Suppl.* **205-206** (2010) 10 [arXiv:1007.3492] [INSPIRE].

JHEP03(2016)127

[69] G. Bevilacqua et al., *HELAC-NLO*, *Comput. Phys. Commun.* **184** (2013) 986 [arXiv:1110.1499] [INSPIRE].

[70] M.V. Garzelli, A. Kardos, C.G. Papadopoulos and Z. Trócsányi, *Standard Model Higgs boson production in association with a top anti-top pair at NLO with parton showering*, *Europhys. Lett.* **96** (2011) 11001 [arXiv:1108.0387] [INSPIRE].

[71] T. Sjöstrand, S. Mrenna and P.Z. Skands, *A Brief Introduction to PYTHIA 8.1*, *Comput. Phys. Commun.* **178** (2008) 852 [arXiv:0710.3820] [INSPIRE].

[72] ATLAS collaboration, *Summary of ATLAS PYTHIA 8 tunes*, ATL-PHYS-PUB-2012-003 (2012).

[73] LHC Higgs Cross Section Working Group, S. Dittmaier et al., *Handbook of LHC Higgs Cross Sections: 1. Inclusive Observables*, arXiv:1101.0593 [INSPIRE].

[74] Z. Was and P. Golonka, *TAUOLA as tau Monte Carlo for future applications*, *Nucl. Phys. Proc. Suppl.* **144** (2005) 88 [hep-ph/0411377] [INSPIRE].

[75] E. Barberio, B. van Eijk and Z. Was, *PHOTOS: A Universal Monte Carlo for QED radiative corrections in decays*, *Comput. Phys. Commun.* **66** (1991) 115 [INSPIRE].

[76] N. Davidson, T. Przedzinski and Z. Was, *PHOTOS Interface in C++: Technical and Physics Documentation*, *Comput. Phys. Commun.* **199** (2016) 86 [arXiv:1011.0937] [INSPIRE].

[77] ATLAS collaboration, *The ATLAS Simulation Infrastructure*, *Eur. Phys. J.* **C 70** (2010) 823 [arXiv:1005.4568] [INSPIRE].

[78] GEANT4 collaboration, S. Agostinelli et al., *GEANT4: A Simulation toolkit*, *Nucl. Instrum. Meth.* **A 506** (2003) 250 [INSPIRE].

[79] ATLAS collaboration, *The simulation principle and performance of the ATLAS fast calorimeter simulation FastCaloSim*, ATL-PHYS-PUB-2010-013 (2010).

[80] ATLAS collaboration, *Electron reconstruction and identification efficiency measurements with the ATLAS detector using the 2011 LHC proton-proton collision data*, *Eur. Phys. J.* **C 74** (2014) 2941 [arXiv:1404.2240] [INSPIRE].

[81] ATLAS collaboration, *Measurement of the muon reconstruction performance of the ATLAS detector using 2011 and 2012 LHC proton-proton collision data*, *Eur. Phys. J.* **C 74** (2014) 3130 [arXiv:1407.3935] [INSPIRE].

[82] L. Lampl, *Calorimeter Clustering Algorithms : Description and Performance*, ATL-LARG-PUB-2008-002 (2008).

[83] M. Cacciari, G.P. Salam and G. Soyez, *The Anti-k_t jet clustering algorithm*, *JHEP* **04** (2008) 063 [arXiv:0802.1189] [INSPIRE].

[84] M. Cacciari and G.P. Salam, *Dispelling the N^3 myth for the k_t jet-finder*, *Phys. Lett.* **B 641** (2006) 57 [hep-ph/0512210] [INSPIRE].

[85] ATLAS collaboration, *Jet energy measurement and its systematic uncertainty in proton-proton collisions at $\sqrt{s} = 7$ TeV with the ATLAS detector*, *Eur. Phys. J.* **C 75** (2015) 17 [arXiv:1406.0076] [INSPIRE].

[86] ATLAS collaboration, *Pile-up subtraction and suppression for jets in ATLAS*, ATLAS-CONF-2013-083 (2013).

[87] ATLAS collaboration, *Measurement of the b-tag Efficiency in a Sample of Jets Containing Muons with 5 fb^{-1} of Data from the ATLAS Detector*, ATLAS-CONF-2012-043 (2012).

JHEP03(2016)127

[88] ATLAS collaboration, *Calibration of b-tagging using dileptonic top pair events in a combinatorial likelihood approach with the ATLAS experiment*, ATLAS-CONF-2014-004 (2014).

[89] ATLAS collaboration, *Performance of jet substructure techniques for large-R jets in proton-proton collisions at $\sqrt{s} = 7$ TeV using the ATLAS detector*, *JHEP* **09** (2013) 076 [arXiv:1306.4945] [INSPIRE].

[90] D. Krohn, J. Thaler and L.-T. Wang, *Jet Trimming*, *JHEP* **02** (2010) 084 [arXiv:0912.1342] [INSPIRE].

[91] S.D. Ellis and D.E. Soper, *Successive combination jet algorithm for hadron collisions*, *Phys. Rev.* **D 48** (1993) 3160 [hep-ph/9305266] [INSPIRE].

[92] J. Thaler and K. Van Tilburg, *Identifying Boosted Objects with N-subjettiness*, *JHEP* **03** (2011) 015 [arXiv:1011.2268] [INSPIRE].

[93] J. Thaler and K. Van Tilburg, *Maximizing Boosted Top Identification by Minimizing N-subjettiness*, *JHEP* **02** (2012) 093 [arXiv:1108.2701] [INSPIRE].

[94] ATLAS collaboration, *Performance of Missing Transverse Momentum Reconstruction in Proton-Proton Collisions at 7 TeV with ATLAS*, *Eur. Phys. J.* **C 72** (2012) 1844 [arXiv:1108.5602] [INSPIRE].

[95] M. Carena, S. Heinemeyer, O. Stål, C.E.M. Wagner and G. Weiglein, *MSSM Higgs Boson Searches at the LHC: Benchmark Scenarios after the Discovery of a Higgs-like Particle*, *Eur. Phys. J.* **C 73** (2013) 2552 [arXiv:1302.7033] [INSPIRE].

[96] M. Flechl, R. Klees, M. Krämer, M. Spira and M. Ubiali, *Improved cross-section predictions for heavy charged Higgs boson production at the LHC*, *Phys. Rev.* **D 91** (2015) 075015 [arXiv:1409.5615] [INSPIRE].

[97] S. Dittmaier, M. Krämer, M. Spira and M. Walser, *Charged-Higgs-boson production at the LHC: NLO supersymmetric QCD corrections*, *Phys. Rev.* **D 83** (2011) 055005 [arXiv:0906.2648] [INSPIRE].

[98] E.L. Berger, T. Han, J. Jiang and T. Plehn, *Associated production of a top quark and a charged Higgs boson*, *Phys. Rev.* **D 71** (2005) 115012 [hep-ph/0312286] [INSPIRE].

[99] A. Höcker et al., *TMVA — Toolkit for Multivariate Data Analysis*, PoS(ACAT)040 [physics/0703039].

[100] C. Bernaciak, M.S.A. Buschmann, A. Butter and T. Plehn, *Fox-Wolfram Moments in Higgs Physics*, *Phys. Rev.* **D 87** (2013) 073014 [arXiv:1212.4436] [INSPIRE].

[101] M. Botje et al., *The PDF4LHC Working Group Interim Recommendations*, arXiv:1101.0538 [INSPIRE].

[102] R.D. Ball et al., *Parton distributions with LHC data*, *Nucl. Phys.* **B 867** (2013) 244 [arXiv:1207.1303] [INSPIRE].

[103] M.L. Mangano, M. Moretti and R. Pittau, *Multijet matrix elements and shower evolution in hadronic collisions: $Wb\bar{b} + n$ jets as a case study*, *Nucl. Phys.* **B 632** (2002) 343 [hep-ph/0108069] [INSPIRE].

[104] S. Frixione and B.R. Webber, *Matching NLO QCD computations and parton shower simulations*, *JHEP* **06** (2002) 029 [hep-ph/0204244] [INSPIRE].

JHEP03(2016)127

[105] M. Bähr et al., *HERWIG++ Physics and Manual*, *Eur. Phys. J.* **C 58** (2008) 639 [arXiv:0803.0883] [INSPIRE].

[106] J. Alwall et al., *The automated computation of tree-level and next-to-leading order differential cross sections and their matching to parton shower simulations*, *JHEP* **07** (2014) 079 [arXiv:1405.0301] [INSPIRE].

[107] ATLAS collaboration, *Combined search for the Standard Model Higgs boson in pp collisions at* $\sqrt{s} = 7$ *TeV with the ATLAS detector*, *Phys. Rev.* **D 86** (2012) 032003 [arXiv:1207.0319] [INSPIRE].

[108] A.L. Read, *Presentation of search results: The* CL_S *technique*, *J. Phys.* **G 28** (2002) 2693 [INSPIRE].

[109] G. Cowan, K. Cranmer, E. Gross and O. Vitells, *Asymptotic formulae for likelihood-based tests of new physics*, *Eur. Phys. J.* **C 71** (2011) 1554 [*Erratum ibid.* **C 73** (2013) 2501] [arXiv:1007.1727] [INSPIRE].

[110] ATLAS collaboration, *Measurement of the t-channel single top-quark production cross section in pp collisions at* $\sqrt{s} = 7$ *TeV with the ATLAS detector*, *Phys. Lett.* **B 717** (2012) 330 [arXiv:1205.3130] [INSPIRE].

[111] A. Buckley et al., *LHAPDF6: parton density access in the LHC precision era*, *Eur. Phys. J.* **C 75** (2015) 132 [arXiv:1412.7420] [INSPIRE].

JHEP03(2016)127

The ATLAS collaboration

G. Aad[85], B. Abbott[113], J. Abdallah[151], O. Abdinov[11], R. Aben[107], M. Abolins[90], O.S. AbouZeid[158], H. Abramowicz[153], H. Abreu[152], R. Abreu[116], Y. Abulaiti[146a,146b], B.S. Acharya[164a,164b,a], L. Adamczyk[38a], D.L. Adams[25], J. Adelman[108], S. Adomeit[100], T. Adye[131], A.A. Affolder[74], T. Agatonovic-Jovin[13], J. Agricola[54], J.A. Aguilar-Saavedra[126a,126f], S.P. Ahlen[22], F. Ahmadov[65,b], G. Aielli[133a,133b], H. Akerstedt[146a,146b], T.P.A. Åkesson[81], A.V. Akimov[96], G.L. Alberghi[20a,20b], J. Albert[169], S. Albrand[55], M.J. Alconada Verzini[71], M. Aleksa[30], I.N. Aleksandrov[65], C. Alexa[26b], G. Alexander[153], T. Alexopoulos[10], M. Alhroob[113], G. Alimonti[91a], L. Alio[85], J. Alison[31], S.P. Alkire[35], B.M.M. Allbrooke[149], P.P. Allport[18], A. Aloisio[104a,104b], A. Alonso[36], F. Alonso[71], C. Alpigiani[138], B. Alvarez Gonzalez[30], D. Álvarez Piqueras[167], M.G. Alviggi[104a,104b], B.T. Amadio[15], K. Amako[66], Y. Amaral Coutinho[24a], C. Amelung[23], D. Amidei[89], S.P. Amor Dos Santos[126a,126c], A. Amorim[126a,126b], S. Amoroso[48], N. Amram[153], G. Amundsen[23], C. Anastopoulos[139], L.S. Ancu[49], N. Andari[108], T. Andeen[31], C.F. Anders[58b], G. Anders[30], J.K. Anders[74], K.J. Anderson[31], A. Andreazza[91a,91b], V. Andrei[58a], S. Angelidakis[9], I. Angelozzi[107], P. Anger[44], A. Angerami[35], F. Anghinolfi[30], A.V. Anisenkov[109,c], N. Anjos[12], A. Annovi[124a,124b], M. Antonelli[47], A. Antonov[98], J. Antos[144b], F. Anulli[132a], M. Aoki[66], L. Aperio Bella[18], G. Arabidze[90], Y. Arai[66], J.P. Araque[126a], A.T.H. Arce[45], F.A. Arduh[71], J-F. Arguin[95], S. Argyropoulos[63], M. Arik[19a], A.J. Armbruster[30], O. Arnaez[30], H. Arnold[48], M. Arratia[28], O. Arslan[21], A. Artamonov[97], G. Artoni[120], S. Artz[83], S. Asai[155], N. Asbah[42], A. Ashkenazi[153], B. Åsman[146a,146b], L. Asquith[149], K. Assamagan[25], R. Astalos[144a], M. Atkinson[165], N.B. Atlay[141], K. Augsten[128], M. Aurousseau[145b], G. Avolio[30], B. Axen[15], M.K. Ayoub[117], G. Azuelos[95,d], M.A. Baak[30], A.E. Baas[58a], M.J. Baca[18], H. Bachacou[136], K. Bachas[154], M. Backes[30], M. Backhaus[30], P. Bagiacchi[132a,132b], P. Bagnaia[132a,132b], Y. Bai[33a], J.T. Baines[131], O.K. Baker[176], E.M. Baldin[109,c], P. Balek[129], T. Balestri[148], F. Balli[84], W.K. Balunas[122], E. Banas[39], Sw. Banerjee[173,e], A.A.E. Bannoura[175], L. Barak[30], E.L. Barberio[88], D. Barberis[50a,50b], M. Barbero[85], T. Barillari[101], M. Barisonzi[164a,164b], T. Barklow[143], N. Barlow[28], S.L. Barnes[84], B.M. Barnett[131], R.M. Barnett[15], Z. Barnovska[5], A. Baroncelli[134a], G. Barone[23], A.J. Barr[120], F. Barreiro[82], J. Barreiro Guimarães da Costa[33a], R. Bartoldus[143], A.E. Barton[72], P. Bartos[144a], A. Basalaev[123], A. Bassalat[117], A. Basye[165], R.L. Bates[53], S.J. Batista[158], J.R. Batley[28], M. Battaglia[137], M. Bauce[132a,132b], F. Bauer[136], H.S. Bawa[143,f], J.B. Beacham[111], M.D. Beattie[72], T. Beau[80], P.H. Beauchemin[161], R. Beccherle[124a,124b], P. Bechtle[21], H.P. Beck[17,g], K. Becker[120], M. Becker[83], M. Beckingham[170], C. Becot[117], A.J. Beddall[19b], A. Beddall[19b], V.A. Bednyakov[65], C.P. Bee[148], L.J. Beemster[107], T.A. Beermann[30], M. Begel[25], J.K. Behr[120], C. Belanger-Champagne[87], W.H. Bell[49], G. Bella[153], L. Bellagamba[20a], A. Bellerive[29], M. Bellomo[86], K. Belotskiy[98], O. Beltramello[30], O. Benary[153], D. Benchekroun[135a], M. Bender[100], K. Bendtz[146a,146b], N. Benekos[10], Y. Benhammou[153], E. Benhar Noccioli[176], J.A. Benitez Garcia[159b], D.P. Benjamin[45], J.R. Bensinger[23], S. Bentvelsen[107], L. Beresford[120], M. Beretta[47], D. Berge[107], E. Bergeaas Kuutmann[166], N. Berger[5], F. Berghaus[169], J. Beringer[15], C. Bernard[22], N.R. Bernard[86], C. Bernius[110], F.U. Bernlochner[21], T. Berry[77], P. Berta[129], C. Bertella[83], G. Bertoli[146a,146b], F. Bertolucci[124a,124b], C. Bertsche[113], D. Bertsche[113], G.J. Besjes[36], O. Bessidskaia Bylund[146a,146b], M. Bessner[42], N. Besson[136], C. Betancourt[48], S. Bethke[101], A.J. Bevan[76], W. Bhimji[15], R.M. Bianchi[125], L. Bianchini[23], M. Bianco[30], O. Biebel[100], D. Biedermann[16], N.V. Biesuz[124a,124b], M. Biglietti[134a], J. Bilbao De Mendizabal[49], H. Bilokon[47], M. Bindi[54], S. Binet[117], A. Bingul[19b], C. Bini[132a,132b], S. Biondi[20a,20b], D.M. Bjergaard[45], C.W. Black[150], J.E. Black[143], K.M. Black[22], D. Blackburn[138], R.E. Blair[6], J.-B. Blanchard[136],

JHEP03(2016)127

J.E. Blanco[77], T. Blazek[144a], I. Bloch[42], C. Blocker[23], W. Blum[83,*], U. Blumenschein[54], S. Blunier[32a], G.J. Bobbink[107], V.S. Bobrovnikov[109,c], S.S. Bocchetta[81], A. Bocci[45], C. Bock[100], M. Boehler[48], J.A. Bogaerts[30], D. Bogavac[13], A.G. Bogdanchikov[109], C. Bohm[146a], V. Boisvert[77], T. Bold[38a], V. Boldea[26b], A.S. Boldyrev[99], M. Bomben[80], M. Bona[76], M. Boonekamp[136], A. Borisov[130], G. Borissov[72], S. Borroni[42], J. Bortfeldt[100], V. Bortolotto[60a,60b,60c], K. Bos[107], D. Boscherini[20a], M. Bosman[12], J. Boudreau[125], J. Bouffard[2], E.V. Bouhova-Thacker[72], D. Boumediene[34], C. Bourdarios[117], N. Bousson[114], S.K. Boutle[53], A. Boveia[30], J. Boyd[30], I.R. Boyko[65], J. Bracinik[18], A. Brandt[8], G. Brandt[54], O. Brandt[58a], U. Bratzler[156], B. Brau[86], J.E. Brau[116], H.M. Braun[175,*], W.D. Breaden Madden[53], K. Brendlinger[122], A.J. Brennan[88], L. Brenner[107], R. Brenner[166], S. Bressler[172], T.M. Bristow[46], D. Britton[53], D. Britzger[42], F.M. Brochu[28], I. Brock[21], R. Brock[90], G. Brooijmans[35], T. Brooks[77], W.K. Brooks[32b], J. Brosamer[15], E. Brost[116], P.A. Bruckman de Renstrom[39], D. Bruncko[144b], R. Bruneliere[48], A. Bruni[20a], G. Bruni[20a], M. Bruschi[20a], N. Bruscino[21], L. Bryngemark[81], T. Buanes[14], Q. Buat[142], P. Buchholz[141], A.G. Buckley[53], I.A. Budagov[65], F. Buehrer[48], L. Bugge[119], M.K. Bugge[119], O. Bulekov[98], D. Bullock[8], H. Burckhart[30], S. Burdin[74], C.D. Burgard[48], B. Burghgrave[108], S. Burke[131], I. Burmeister[43], E. Busato[34], D. Büscher[48], V. Büscher[83], P. Bussey[53], J.M. Butler[22], A.I. Butt[3], C.M. Buttar[53], J.M. Butterworth[78], P. Butti[107], W. Buttinger[25], A. Buzatu[53], A.R. Buzykaev[109,c], S. Cabrera Urbán[167], D. Caforio[128], V.M. Cairo[37a,37b], O. Cakir[4a], N. Calace[49], P. Calafiura[15], A. Calandri[136], G. Calderini[80], P. Calfayan[100], L.P. Caloba[24a], D. Calvet[34], S. Calvet[34], R. Camacho Toro[31], S. Camarda[42], P. Camarri[133a,133b], D. Cameron[119], R. Caminal Armadans[165], S. Campana[30], M. Campanelli[78], A. Campoverde[148], V. Canale[104a,104b], A. Canepa[159a], M. Cano Bret[33e], J. Cantero[82], R. Cantrill[126a], T. Cao[40], M.D.M. Capeans Garrido[30], I. Caprini[26b], M. Caprini[26b], M. Capua[37a,37b], R. Caputo[83], R.M. Carbone[35], R. Cardarelli[133a], F. Cardillo[48], T. Carli[30], G. Carlino[104a], L. Carminati[91a,91b], S. Caron[106], E. Carquin[32a], G.D. Carrillo-Montoya[30], J.R. Carter[28], J. Carvalho[126a,126c], D. Casadei[78], M.P. Casado[12], M. Casolino[12], D.W. Casper[163], E. Castaneda-Miranda[145a], A. Castelli[107], V. Castillo Gimenez[167], N.F. Castro[126a,h], P. Catastini[57], A. Catinaccio[30], J.R. Catmore[119], A. Cattai[30], J. Caudron[83], V. Cavaliere[165], D. Cavalli[91a], M. Cavalli-Sforza[12], V. Cavasinni[124a,124b], F. Ceradini[134a,134b], L. Cerda Alberich[167], B.C. Cerio[45], A.S. Cerqueira[24b], A. Cerri[149], L. Cerrito[76], F. Cerutti[15], M. Cerv[30], A. Cervelli[17], S.A. Cetin[19c], A. Chafaq[135a], D. Chakraborty[108], I. Chalupkova[129], Y.L. Chan[60a], P. Chang[165], J.D. Chapman[28], D.G. Charlton[18], C.C. Chau[158], C.A. Chavez Barajas[149], S. Che[111], S. Cheatham[152], A. Chegwidden[90], S. Chekanov[6], S.V. Chekulaev[159a], G.A. Chelkov[65,i], M.A. Chelstowska[89], C. Chen[64], H. Chen[25], K. Chen[148], L. Chen[33d,j], S. Chen[33c], S. Chen[155], X. Chen[33f], Y. Chen[67], H.C. Cheng[89], Y. Cheng[31], A. Cheplakov[65], E. Cheremushkina[130], R. Cherkaoui El Moursli[135e], V. Chernyatin[25,*], E. Cheu[7], L. Chevalier[136], V. Chiarella[47], G. Chiarelli[124a,124b], G. Chiodini[73a], A.S. Chisholm[18], R.T. Chislett[78], A. Chitan[26b], M.V. Chizhov[65], K. Choi[61], S. Chouridou[9], B.K.B. Chow[100], V. Christodoulou[78], D. Chromek-Burckhart[30], J. Chudoba[127], A.J. Chuinard[87], J.J. Chwastowski[39], L. Chytka[115], G. Ciapetti[132a,132b], A.K. Ciftci[4a], D. Cinca[53], V. Cindro[75], I.A. Cioara[21], A. Ciocio[15], F. Cirotto[104a,104b], Z.H. Citron[172], M. Ciubancan[26b], A. Clark[49], B.L. Clark[57], P.J. Clark[46], R.N. Clarke[15], C. Clement[146a,146b], Y. Coadou[85], M. Cobal[164a,164c], A. Coccaro[49], J. Cochran[64], L. Coffey[23], H. Cohen[153], L. Colasurdo[106], B. Cole[35], S. Cole[108], A.P. Colijn[107], J. Collot[55], T. Colombo[58c], G. Compostella[101], P. Conde Muiño[126a,126b], E. Coniavitis[48], S.H. Connell[145b], I.A. Connelly[77], V. Consorti[48], S. Constantinescu[26b], C. Conta[121a,121b], G. Conti[30], F. Conventi[104a,k], M. Cooke[15], B.D. Cooper[78], A.M. Cooper-Sarkar[120], T. Cornelissen[175], M. Corradi[132a,132b], F. Corriveau[87,l], A. Corso-Radu[163], A. Cortes-Gonzalez[12], G. Cortiana[101], G. Costa[91a], M.J. Costa[167],

JHEP03(2016)127

D. Costanzo[139], D. Côté[8], G. Cottin[28], G. Cowan[77], B.E. Cox[84], K. Cranmer[110], S.J. Crawley[53], G. Cree[29], S. Crépé-Renaudin[55], F. Crescioli[80], W.A. Cribbs[146a,146b], M. Crispin Ortuzar[120], M. Cristinziani[21], V. Croft[106], G. Crosetti[37a,37b], T. Cuhadar Donszelmann[139], J. Cummings[176], M. Curatolo[47], J. Cúth[83], C. Cuthbert[150], H. Czirr[141], P. Czodrowski[3], S. D'Auria[53], M. D'Onofrio[74], M.J. Da Cunha Sargedas De Sousa[126a,126b], C. Da Via[84], W. Dabrowski[38a], A. Dafinca[120], T. Dai[89], O. Dale[14], F. Dallaire[95], C. Dallapiccola[86], M. Dam[36], J.R. Dandoy[31], N.P. Dang[48], A.C. Daniells[18], M. Danninger[168], M. Dano Hoffmann[136], V. Dao[48], G. Darbo[50a], S. Darmora[8], J. Dassoulas[3], A. Dattagupta[61], W. Davey[21], C. David[169], T. Davidek[129], E. Davies[120,m], M. Davies[153], P. Davison[78], Y. Davygora[58a], E. Dawe[88], I. Dawson[139], R.K. Daya-Ishmukhametova[86], K. De[8], R. de Asmundis[104a], A. De Benedetti[113], S. De Castro[20a,20b], S. De Cecco[80], N. De Groot[106], P. de Jong[107], H. De la Torre[82], F. De Lorenzi[64], D. De Pedis[132a], A. De Salvo[132a], U. De Sanctis[149], A. De Santo[149], J.B. De Vivie De Regie[117], W.J. Dearnaley[72], R. Debbe[25], C. Debenedetti[137], D.V. Dedovich[65], I. Deigaard[107], J. Del Peso[82], T. Del Prete[124a,124b], D. Delgove[117], F. Deliot[136], C.M. Delitzsch[49], M. Deliyergiyev[75], A. Dell'Acqua[30], L. Dell'Asta[22], M. Dell'Orso[124a,124b], M. Della Pietra[104a,k], D. della Volpe[49], M. Delmastro[5], P.A. Delsart[55], C. Deluca[107], D.A. DeMarco[158], S. Demers[176], M. Demichev[65], A. Demilly[80], S.P. Denisov[130], D. Denysiuk[136], D. Derendarz[39], J.E. Derkaoui[135d], F. Derue[80], P. Dervan[74], K. Desch[21], C. Deterre[42], K. Dette[43], P.O. Deviveiros[30], A. Dewhurst[131], S. Dhaliwal[23], A. Di Ciaccio[133a,133b], L. Di Ciaccio[5], A. Di Domenico[132a,132b], C. Di Donato[132a,132b], A. Di Girolamo[30], B. Di Girolamo[30], A. Di Mattia[152], B. Di Micco[134a,134b], R. Di Nardo[47], A. Di Simone[48], R. Di Sipio[158], D. Di Valentino[29], C. Diaconu[85], M. Diamond[158], F.A. Dias[46], M.A. Diaz[32a], E.B. Diehl[89], J. Dietrich[16], S. Diglio[85], A. Dimitrievska[13], J. Dingfelder[21], P. Dita[26b], S. Dita[26b], F. Dittus[30], F. Djama[85], T. Djobava[51b], J.I. Djuvsland[58a], M.A.B. do Vale[24c], D. Dobos[30], M. Dobre[26b], C. Doglioni[81], T. Dohmae[155], J. Dolejsi[129], Z. Dolezal[129], B.A. Dolgoshein[98,*], M. Donadelli[24d], S. Donati[124a,124b], P. Dondero[121a,121b], J. Donini[34], J. Dopke[131], A. Doria[104a], M.T. Dova[71], A.T. Doyle[53], E. Drechsler[54], M. Dris[10], Y. Du[33d], J. Duarte-Campderros[153], E. Dubreuil[34], E. Duchovni[172], G. Duckeck[100], O.A. Ducu[26b,85], D. Duda[107], A. Dudarev[30], L. Duflot[117], L. Duguid[77], M. Dührssen[30], M. Dunford[58a], H. Duran Yildiz[4a], M. Düren[52], A. Durglishvili[51b], D. Duschinger[44], B. Dutta[42], M. Dyndal[38a], C. Eckardt[42], K.M. Ecker[101], R.C. Edgar[89], W. Edson[2], N.C. Edwards[46], W. Ehrenfeld[21], T. Eifert[30], G. Eigen[14], K. Einsweiler[15], T. Ekelof[166], M. El Kacimi[135c], M. Ellert[166], S. Elles[5], F. Ellinghaus[175], A.A. Elliot[169], N. Ellis[30], J. Elmsheuser[100], M. Elsing[30], D. Emeliyanov[131], Y. Enari[155], O.C. Endner[83], M. Endo[118], J. Erdmann[43], A. Ereditato[17], G. Ernis[175], J. Ernst[2], M. Ernst[25], S. Errede[165], E. Ertel[83], M. Escalier[117], H. Esch[43], C. Escobar[125], B. Esposito[47], A.I. Etienvre[136], E. Etzion[153], H. Evans[61], A. Ezhilov[123], L. Fabbri[20a,20b], G. Facini[31], R.M. Fakhrutdinov[130], S. Falciano[132a], R.J. Falla[78], J. Faltova[129], Y. Fang[33a], M. Fanti[91a,91b], A. Farbin[8], A. Farilla[134a], T. Farooque[12], S. Farrell[15], S.M. Farrington[170], P. Farthouat[30], F. Fassi[135e], P. Fassnacht[30], D. Fassouliotis[9], M. Faucci Giannelli[77], A. Favareto[50a,50b], L. Fayard[117], O.L. Fedin[123,n], W. Fedorko[168], S. Feigl[119], L. Feligioni[85], C. Feng[33d], E.J. Feng[30], H. Feng[89], A.B. Fenyuk[130], L. Feremenga[8], P. Fernandez Martinez[167], S. Fernandez Perez[12], J. Ferrando[53], A. Ferrari[166], P. Ferrari[107], R. Ferrari[121a], D.E. Ferreira de Lima[53], A. Ferrer[167], D. Ferrere[49], C. Ferretti[89], A. Ferretto Parodi[50a,50b], F. Fiedler[83], A. Filipčič[75], M. Filipuzzi[42], F. Filthaut[106], M. Fincke-Keeler[169], K.D. Finelli[150], M.C.N. Fiolhais[126a,126c], L. Fiorini[167], A. Firan[40], A. Fischer[2], C. Fischer[12], J. Fischer[175], W.C. Fisher[90], N. Flaschel[42], I. Fleck[141], P. Fleischmann[89], G.T. Fletcher[139], G. Fletcher[76], R.R.M. Fletcher[122], T. Flick[175], A. Floderus[81], L.R. Flores Castillo[60a], M.J. Flowerdew[101], G.T. Forcolin[84], A. Formica[136], A. Forti[84], D. Fournier[117], H. Fox[72], S. Fracchia[12], P. Francavilla[80], M. Franchini[20a,20b], D. Francis[30],

JHEP03(2016)127

L. Franconi[119], M. Franklin[57], M. Frate[163], M. Fraternali[121a,121b], D. Freeborn[78], S.T. French[28], S.M. Fressard-Batraneanu[30], F. Friedrich[44], D. Froidevaux[30], J.A. Frost[120], C. Fukunaga[156], E. Fullana Torregrosa[83], T. Fusayasu[102], J. Fuster[167], C. Gabaldon[55], O. Gabizon[175], A. Gabrielli[20a,20b], A. Gabrielli[15], G.P. Gach[18], S. Gadatsch[30], S. Gadomski[49], G. Gagliardi[50a,50b], P. Gagnon[61], C. Galea[106], B. Galhardo[126a,126c], E.J. Gallas[120], B.J. Gallop[131], P. Gallus[128], G. Galster[36], K.K. Gan[111], J. Gao[33b,85], Y. Gao[46], Y.S. Gao[143,f], F.M. Garay Walls[46], C. García[167], J.E. García Navarro[167], M. Garcia-Sciveres[15], R.W. Gardner[31], N. Garelli[143], V. Garonne[119], C. Gatti[47], A. Gaudiello[50a,50b], G. Gaudio[121a], B. Gaur[141], L. Gauthier[95], I.L. Gavrilenko[96], C. Gay[168], G. Gaycken[21], E.N. Gazis[10], Z. Gecse[168], C.N.P. Gee[131], Ch. Geich-Gimbel[21], M.P. Geisler[58a], C. Gemme[50a], M.H. Genest[55], C. Geng[33b,o], S. Gentile[132a,132b], S. George[77], D. Gerbaudo[163], A. Gershon[153], S. Ghasemi[141], H. Ghazlane[135b], B. Giacobbe[20a], S. Giagu[132a,132b], P. Giannetti[124a,124b], B. Gibbard[25], S.M. Gibson[77], M. Gignac[168], M. Gilchriese[15], T.P.S. Gillam[28], D. Gillberg[30], G. Gilles[34], D.M. Gingrich[3,d], N. Giokaris[9], M.P. Giordani[164a,164c], F.M. Giorgi[20a], F.M. Giorgi[16], P.F. Giraud[136], P. Giromini[57], D. Giugni[91a], C. Giuliani[101], M. Giulini[58b], B.K. Gjelsten[119], S. Gkaitatzis[154], I. Gkialas[154], E.L. Gkougkousis[117], L.K. Gladilin[99], C. Glasman[82], J. Glatzer[30], P.C.F. Glaysher[46], A. Glazov[42], M. Goblirsch-Kolb[101], J.R. Goddard[76], J. Godlewski[39], S. Goldfarb[89], T. Golling[49], D. Golubkov[130], A. Gomes[126a,126b,126d], R. Gonçalo[126a], J. Goncalves Pinto Firmino Da Costa[136], L. Gonella[21], S. González de la Hoz[167], G. Gonzalez Parra[12], S. Gonzalez-Sevilla[49], L. Goossens[30], P.A. Gorbounov[97], H.A. Gordon[25], I. Gorelov[105], B. Gorini[30], E. Gorini[73a,73b], A. Gorišek[75], E. Gornicki[39], A.T. Goshaw[45], C. Gössling[43], M.I. Gostkin[65], D. Goujdami[135c], A.G. Goussiou[138], N. Govender[145b], E. Gozani[152], L. Graber[54], I. Grabowska-Bold[38a], P.O.J. Gradin[166], P. Grafström[20a,20b], J. Gramling[49], E. Gramstad[119], S. Grancagnolo[16], V. Gratchev[123], H.M. Gray[30], E. Graziani[134a], Z.D. Greenwood[79,p], C. Grefe[21], K. Gregersen[78], I.M. Gregor[42], P. Grenier[143], J. Griffiths[8], A.A. Grillo[137], K. Grimm[72], S. Grinstein[12,q], Ph. Gris[34], J.-F. Grivaz[117], S. Groh[83], J.P. Grohs[44], A. Grohsjean[42], E. Gross[172], J. Grosse-Knetter[54], G.C. Grossi[79], Z.J. Grout[149], L. Guan[89], J. Guenther[128], F. Guescini[49], D. Guest[163], O. Gueta[153], E. Guido[50a,50b], T. Guillemin[5], S. Guindon[2], U. Gul[53], C. Gumpert[30], J. Guo[33e], Y. Guo[33b,o], S. Gupta[120], G. Gustavino[132a,132b], P. Gutierrez[113], N.G. Gutierrez Ortiz[78], C. Gutschow[44], C. Guyot[136], C. Gwenlan[120], C.B. Gwilliam[74], A. Haas[110], C. Haber[15], H.K. Hadavand[8], N. Haddad[135e], P. Haefner[21], S. Hageböck[21], Z. Hajduk[39], H. Hakobyan[177], M. Haleem[42], J. Haley[114], D. Hall[120], G. Halladjian[90], G.D. Hallewell[85], K. Hamacher[175], P. Hamal[115], K. Hamano[169], A. Hamilton[145a], G.N. Hamity[139], P.G. Hamnett[42], L. Han[33b], K. Hanagaki[66,r], K. Hanawa[155], M. Hance[137], B. Haney[122], P. Hanke[58a], R. Hanna[136], J.B. Hansen[36], J.D. Hansen[36], M.C. Hansen[21], P.H. Hansen[36], K. Hara[160], A.S. Hard[173], T. Harenberg[175], F. Hariri[117], S. Harkusha[92], R.D. Harrington[46], P.F. Harrison[170], F. Hartjes[107], M. Hasegawa[67], Y. Hasegawa[140], A. Hasib[113], S. Hassani[136], S. Haug[17], R. Hauser[90], L. Hauswald[44], M. Havranek[127], C.M. Hawkes[18], R.J. Hawkings[30], A.D. Hawkins[81], T. Hayashi[160], D. Hayden[90], C.P. Hays[120], J.M. Hays[76], H.S. Hayward[74], S.J. Haywood[131], S.J. Head[18], T. Heck[83], V. Hedberg[81], L. Heelan[8], S. Heim[122], T. Heim[15], B. Heinemann[15], L. Heinrich[110], J. Hejbal[127], L. Helary[22], S. Hellman[146a,146b], C. Helsens[30], J. Henderson[120], R.C.W. Henderson[72], Y. Heng[173], S. Henkelmann[168], A.M. Henriques Correia[30], S. Henrot-Versille[117], G.H. Herbert[16], Y. Hernández Jiménez[167], G. Herten[48], R. Hertenberger[100], L. Hervas[30], G.G. Hesketh[78], N.P. Hessey[107], J.W. Hetherly[40], R. Hickling[76], E. Higón-Rodriguez[167], E. Hill[169], J.C. Hill[28], K.H. Hiller[42], S.J. Hillier[18], I. Hinchliffe[15], E. Hines[122], R.R. Hinman[15], M. Hirose[157], D. Hirschbuehl[175], J. Hobbs[148], N. Hod[107], M.C. Hodgkinson[139], P. Hodgson[139], A. Hoecker[30], M.R. Hoeferkamp[105], F. Hoenig[100], M. Hohlfeld[83], D. Hohn[21], T.R. Holmes[15], M. Homann[43], T.M. Hong[125], B.H. Hooberman[165], W.H. Hopkins[116], Y. Horii[103], A.J. Horton[142],

JHEP03(2016)127

J-Y. Hostachy[55], S. Hou[151], A. Hoummada[135a], J. Howard[120], J. Howarth[42], M. Hrabovsky[115], I. Hristova[16], J. Hrivnac[117], T. Hryn'ova[5], A. Hrynevich[93], C. Hsu[145c], P.J. Hsu[151,s], S.-C. Hsu[138], D. Hu[35], Q. Hu[33b], Y. Huang[42], Z. Hubacek[128], F. Hubaut[85], F. Huegging[21], T.B. Huffman[120], E.W. Hughes[35], G. Hughes[72], M. Huhtinen[30], T.A. Hülsing[83], N. Huseynov[65,b], J. Huston[90], J. Huth[57], G. Iacobucci[49], G. Iakovidis[25], I. Ibragimov[141], L. Iconomidou-Fayard[117], E. Ideal[176], Z. Idrissi[135e], P. Iengo[30], O. Igonkina[107], T. Iizawa[171], Y. Ikegami[66], M. Ikeno[66], Y. Ilchenko[31,t], D. Iliadis[154], N. Ilic[143], T. Ince[101], G. Introzzi[121a,121b], P. Ioannou[9], M. Iodice[134a], K. Iordanidou[35], V. Ippolito[57], A. Irles Quiles[167], C. Isaksson[166], M. Ishino[68], M. Ishitsuka[157], R. Ishmukhametov[111], C. Issever[120], S. Istin[19a], J.M. Iturbe Ponce[84], R. Iuppa[133a,133b], J. Ivarsson[81], W. Iwanski[39], H. Iwasaki[66], J.M. Izen[41], V. Izzo[104a], S. Jabbar[3], B. Jackson[122], M. Jackson[74], P. Jackson[1], M.R. Jaekel[30], V. Jain[2], K.B. Jakobi[83], K. Jakobs[48], S. Jakobsen[30], T. Jakoubek[127], J. Jakubek[128], D.O. Jamin[114], D.K. Jana[79], E. Jansen[78], R. Jansky[62], J. Janssen[21], M. Janus[54], G. Jarlskog[81], N. Javadov[65,b], T. Javůrek[48], F. Jeanneau[136], L. Jeanty[15], J. Jejelava[51a,u], G.-Y. Jeng[150], D. Jennens[88], P. Jenni[48,v], J. Jentzsch[43], C. Jeske[170], S. Jézéquel[5], H. Ji[173], J. Jia[148], H. Jiang[64], Y. Jiang[33b], S. Jiggins[78], J. Jimenez Pena[167], S. Jin[33a], A. Jinaru[26b], O. Jinnouchi[157], P. Johansson[139], K.A. Johns[7], W.J. Johnson[138], K. Jon-And[146a,146b], G. Jones[170], R.W.L. Jones[72], T.J. Jones[74], J. Jongmanns[58a], P.M. Jorge[126a,126b], K.D. Joshi[84], J. Jovicevic[159a], X. Ju[173], A. Juste Rozas[12,q], M.K. Köhler[172], M. Kaci[167], A. Kaczmarska[39], M. Kado[117], H. Kagan[111], M. Kagan[143], S.J. Kahn[85], E. Kajomovitz[45], C.W. Kalderon[120], A. Kaluza[83], S. Kama[40], A. Kamenshchikov[130], N. Kanaya[155], S. Kaneti[28], V.A. Kantserov[98], J. Kanzaki[66], B. Kaplan[110], L.S. Kaplan[173], A. Kapliy[31], D. Kar[145c], K. Karakostas[10], A. Karamaoun[3], N. Karastathis[10,107], M.J. Kareem[54], E. Karentzos[10], M. Karnevskiy[83], S.N. Karpov[65], Z.M. Karpova[65], K. Karthik[110], V. Kartvelishvili[72], A.N. Karyukhin[130], K. Kasahara[160], L. Kashif[173], R.D. Kass[111], A. Kastanas[14], Y. Kataoka[155], C. Kato[155], A. Katre[49], J. Katzy[42], K. Kawade[103], K. Kawagoe[70], T. Kawamoto[155], G. Kawamura[54], S. Kazama[155], V.F. Kazanin[109,c], R. Keeler[169], R. Kehoe[40], J.S. Keller[42], J.J. Kempster[77], H. Keoshkerian[84], O. Kepka[127], B.P. Kerševan[75], S. Kersten[175], R.A. Keyes[87], F. Khalil-zada[11], H. Khandanyan[146a,146b], A. Khanov[114], A.G. Kharlamov[109,c], T.J. Khoo[28], V. Khovanskiy[97], E. Khramov[65], J. Khubua[51b,w], S. Kido[67], H.Y. Kim[8], S.H. Kim[160], Y.K. Kim[31], N. Kimura[154], O.M. Kind[16], B.T. King[74], M. King[167], S.B. King[168], J. Kirk[131], A.E. Kiryunin[101], T. Kishimoto[67], D. Kisielewska[38a], F. Kiss[48], K. Kiuchi[160], O. Kivernyk[136], E. Kladiva[144b], M.H. Klein[35], M. Klein[74], U. Klein[74], K. Kleinknecht[83], P. Klimek[146a,146b], A. Klimentov[25], R. Klingenberg[43], J.A. Klinger[139], T. Klioutchnikova[30], E.-E. Kluge[58a], P. Kluit[107], S. Kluth[101], J. Knapik[39], E. Kneringer[62], E.B.F.G. Knoops[85], A. Knue[53], A. Kobayashi[155], D. Kobayashi[157], T. Kobayashi[155], M. Kobel[44], M. Kocian[143], P. Kodys[129], T. Koffas[29], E. Koffeman[107], L.A. Kogan[120], S. Kohlmann[175], Z. Kohout[128], T. Kohriki[66], T. Koi[143], H. Kolanoski[16], M. Kolb[58b], I. Koletsou[5], A.A. Komar[96,*], Y. Komori[155], T. Kondo[66], N. Kondrashova[42], K. Köneke[48], A.C. König[106], T. Kono[66,x], R. Konoplich[110,y], N. Konstantinidis[78], R. Kopeliansky[152], S. Koperny[38a], L. Köpke[83], A.K. Kopp[48], K. Korcyl[39], K. Kordas[154], A. Korn[78], A.A. Korol[109,c], I. Korolkov[12], E.V. Korolkova[139], O. Kortner[101], S. Kortner[101], T. Kosek[129], V.V. Kostyukhin[21], V.M. Kotov[65], A. Kotwal[45], A. Kourkoumeli-Charalampidi[154], C. Kourkoumelis[9], V. Kouskoura[25], A. Koutsman[159a], R. Kowalewski[169], T.Z. Kowalski[38a], W. Kozanecki[136], A.S. Kozhin[130], V.A. Kramarenko[99], G. Kramberger[75], D. Krasnopevtsev[98], M.W. Krasny[80], A. Krasznahorkay[30], J.K. Kraus[21], A. Kravchenko[25], M. Kretz[58c], J. Kretzschmar[74], K. Kreutzfeldt[52], P. Krieger[158], K. Krizka[31], K. Kroeninger[43], H. Kroha[101], J. Kroll[122], J. Kroseberg[21], J. Krstic[13], U. Kruchonak[65], H. Krüger[21], N. Krumnack[64], A. Kruse[173], M.C. Kruse[45], M. Kruskal[22], T. Kubota[88], H. Kucuk[78], S. Kuday[4b], S. Kuehn[48], A. Kugel[58c], F. Kuger[174], A. Kuhl[137], T. Kuhl[42], V. Kukhtin[65],

JHEP03(2016)127

R. Kukla[136], Y. Kulchitsky[92], S. Kuleshov[32b], M. Kuna[132a,132b], T. Kunigo[68], A. Kupco[127], H. Kurashige[67], Y.A. Kurochkin[92], V. Kus[127], E.S. Kuwertz[169], M. Kuze[157], J. Kvita[115], T. Kwan[169], D. Kyriazopoulos[139], A. La Rosa[137], J.L. La Rosa Navarro[24d], L. La Rotonda[37a,37b], C. Lacasta[167], F. Lacava[132a,132b], J. Lacey[29], H. Lacker[16], D. Lacour[80], V.R. Lacuesta[167], E. Ladygin[65], R. Lafaye[5], B. Laforge[80], T. Lagouri[176], S. Lai[54], L. Lambourne[78], S. Lammers[61], C.L. Lampen[7], W. Lampl[7], E. Lançon[136], U. Landgraf[48], M.P.J. Landon[76], V.S. Lang[58a], J.C. Lange[12], A.J. Lankford[163], F. Lanni[25], K. Lantzsch[21], A. Lanza[121a], S. Laplace[80], C. Lapoire[30], J.F. Laporte[136], T. Lari[91a], F. Lasagni Manghi[20a,20b], M. Lassnig[30], P. Laurelli[47], W. Lavrijsen[15], A.T. Law[137], P. Laycock[74], T. Lazovich[57], O. Le Dortz[80], E. Le Guirriec[85], E. Le Menedeu[12], M. LeBlanc[169], T. LeCompte[6], F. Ledroit-Guillon[55], C.A. Lee[145a], S.C. Lee[151], L. Lee[1], G. Lefebvre[80], M. Lefebvre[169], F. Legger[100], C. Leggett[15], A. Lehan[74], G. Lehmann Miotto[30], X. Lei[7], W.A. Leight[29], A. Leisos[154,z], A.G. Leister[176], M.A.L. Leite[24d], R. Leitner[129], D. Lellouch[172], B. Lemmer[54], K.J.C. Leney[78], T. Lenz[21], B. Lenzi[30], R. Leone[7], S. Leone[124a,124b], C. Leonidopoulos[46], S. Leontsinis[10], C. Leroy[95], C.G. Lester[28], M. Levchenko[123], J. Levêque[5], D. Levin[89], L.J. Levinson[172], M. Levy[18], A. Lewis[120], A.M. Leyko[21], M. Leyton[41], B. Li[33b,aa], H. Li[148], H.L. Li[31], L. Li[45], L. Li[33e], S. Li[45], X. Li[84], Y. Li[33c,ab], Z. Liang[137], H. Liao[34], B. Liberti[133a], A. Liblong[158], P. Lichard[30], K. Lie[165], J. Liebal[21], W. Liebig[14], C. Limbach[21], A. Limosani[150], S.C. Lin[151,ac], T.H. Lin[83], B.E. Lindquist[148], J.T. Linnemann[90], E. Lipeles[122], A. Lipniacka[14], M. Lisovyi[58b], T.M. Liss[165], D. Lissauer[25], A. Lister[168], A.M. Litke[137], B. Liu[151,ad], D. Liu[151], H. Liu[89], J. Liu[85], J.B. Liu[33b], K. Liu[85], L. Liu[165], M. Liu[45], M. Liu[33b], Y. Liu[33b], M. Livan[121a,121b], A. Lleres[55], J. Llorente Merino[82], S.L. Lloyd[76], F. Lo Sterzo[151], E. Lobodzinska[42], P. Loch[7], W.S. Lockman[137], F.K. Loebinger[84], A.E. Loevschall-Jensen[36], K.M. Loew[23], A. Loginov[176], T. Lohse[16], K. Lohwasser[42], M. Lokajicek[127], B.A. Long[22], J.D. Long[165], R.E. Long[72], K.A. Looper[111], L. Lopes[126a], D. Lopez Mateos[57], B. Lopez Paredes[139], I. Lopez Paz[12], J. Lorenz[100], N. Lorenzo Martinez[61], M. Losada[162], P.J. Lösel[100], X. Lou[33a], A. Lounis[117], J. Love[6], P.A. Love[72], H. Lu[60a], N. Lu[89], H.J. Lubatti[138], C. Luci[132a,132b], A. Lucotte[55], C. Luedtke[48], F. Luehring[61], W. Lukas[62], L. Luminari[132a], O. Lundberg[146a,146b], B. Lund-Jensen[147], D. Lynn[25], R. Lysak[127], E. Lytken[81], H. Ma[25], L.L. Ma[33d], G. Maccarrone[47], A. Macchiolo[101], C.M. Macdonald[139], B. Maček[75], J. Machado Miguens[122,126b], D. Macina[30], D. Madaffari[85], R. Madar[34], H.J. Maddocks[72], W.F. Mader[44], A. Madsen[42], J. Maeda[67], S. Maeland[14], T. Maeno[25], A. Maevskiy[99], E. Magradze[54], K. Mahboubi[48], J. Mahlstedt[107], C. Maiani[136], C. Maidantchik[24a], A.A. Maier[101], T. Maier[100], A. Maio[126a,126b,126d], S. Majewski[116], Y. Makida[66], N. Makovec[117], B. Malaescu[80], Pa. Malecki[39], V.P. Maleev[123], F. Malek[55], U. Mallik[63], D. Malon[6], C. Malone[143], S. Maltezos[10], V.M. Malyshev[109], S. Malyukov[30], J. Mamuzic[42], G. Mancini[47], B. Mandelli[30], L. Mandelli[91a], I. Mandić[75], J. Maneira[126a,126b], L. Manhaes de Andrade Filho[24b], J. Manjarres Ramos[159b], A. Mann[100], A. Manousakis-Katsikakis[9], B. Mansoulie[136], R. Mantifel[87], M. Mantoani[54], S. Manzoni[91a,91b], L. Mapelli[30], L. March[145c], G. Marchiori[80], M. Marcisovsky[127], M. Marjanovic[13], D.E. Marley[89], F. Marroquim[24a], S.P. Marsden[84], Z. Marshall[15], L.F. Marti[17], S. Marti-Garcia[167], B. Martin[90], T.A. Martin[170], V.J. Martin[46], B. Martin dit Latour[14], M. Martinez[12,q], S. Martin-Haugh[131], V.S. Martoiu[26b], A.C. Martyniuk[78], M. Marx[138], F. Marzano[132a], A. Marzin[30], L. Masetti[83], T. Mashimo[155], R. Mashinistov[96], J. Masik[84], A.L. Maslennikov[109,c], I. Massa[20a,20b], L. Massa[20a,20b], P. Mastrandrea[5], A. Mastroberardino[37a,37b], T. Masubuchi[155], P. Mättig[175], J. Mattmann[83], J. Maurer[26b], S.J. Maxfield[74], D.A. Maximov[109,c], R. Mazini[151], S.M. Mazza[91a,91b], G. Mc Goldrick[158], S.P. Mc Kee[89], A. McCarn[89], R.L. McCarthy[148], T.G. McCarthy[29], K.W. McFarlane[56,*], J.A. Mcfayden[78], G. Mchedlidze[54], S.J. McMahon[131], R.A. McPherson[169,l], M. Medinnis[42], S. Meehan[138], S. Mehlhase[100], A. Mehta[74], K. Meier[58a],

JHEP03(2016)127

C. Meineck[100], B. Meirose[41], B.R. Mellado Garcia[145c], F. Meloni[17], A. Mengarelli[20a,20b], S. Menke[101], E. Meoni[161], K.M. Mercurio[57], S. Mergelmeyer[16], P. Mermod[49], L. Merola[104a,104b], C. Meroni[91a], F.S. Merritt[31], A. Messina[132a,132b], J. Metcalfe[6], A.S. Mete[163], C. Meyer[83], C. Meyer[122], J-P. Meyer[136], J. Meyer[107], H. Meyer Zu Theenhausen[58a], R.P. Middleton[131], S. Miglioranzi[164a,164c], L. Mijović[21], G. Mikenberg[172], M. Mikestikova[127], M. Mikuž[75], M. Milesi[88], A. Milic[30], D.W. Miller[31], C. Mills[46], A. Milov[172], D.A. Milstead[146a,146b], A.A. Minaenko[130], Y. Minami[155], I.A. Minashvili[65], A.I. Mincer[110], B. Mindur[38a], M. Mineev[65], Y. Ming[173], L.M. Mir[12], K.P. Mistry[122], T. Mitani[171], J. Mitrevski[100], V.A. Mitsou[167], A. Miucci[49], P.S. Miyagawa[139], J.U. Mjörnmark[81], T. Moa[146a,146b], K. Mochizuki[85], S. Mohapatra[35], W. Mohr[48], S. Molander[146a,146b], R. Moles-Valls[21], R. Monden[68], M.C. Mondragon[90], K. Mönig[42], C. Monini[55], J. Monk[36], E. Monnier[85], A. Montalbano[148], J. Montejo Berlingen[30], F. Monticelli[71], S. Monzani[132a,132b], R.W. Moore[3], N. Morange[117], D. Moreno[162], M. Moreno Llácer[54], P. Morettini[50a], D. Mori[142], T. Mori[155], M. Morii[57], M. Morinaga[155], V. Morisbak[119], S. Moritz[83], A.K. Morley[150], G. Mornacchi[30], J.D. Morris[76], S.S. Mortensen[36], A. Morton[53], L. Morvaj[148], M. Mosidze[51b], J. Moss[143], K. Motohashi[157], R. Mount[143], E. Mountricha[25], S.V. Mouraviev[96,*], E.J.W. Moyse[86], S. Muanza[85], R.D. Mudd[18], F. Mueller[101], J. Mueller[125], R.S.P. Mueller[100], T. Mueller[28], D. Muenstermann[72], P. Mullen[53], G.A. Mullier[17], F.J. Munoz Sanchez[84], J.A. Murillo Quijada[18], W.J. Murray[170,131], H. Musheghyan[54], A.G. Myagkov[130,ae], M. Myska[128], B.P. Nachman[143], O. Nackenhorst[49], J. Nadal[54], K. Nagai[120], R. Nagai[157], Y. Nagai[85], K. Nagano[66], Y. Nagasaka[59], K. Nagata[160], M. Nagel[101], E. Nagy[85], A.M. Nairz[30], Y. Nakahama[30], K. Nakamura[66], T. Nakamura[155], I. Nakano[112], H. Namasivayam[41], R.F. Naranjo Garcia[42], R. Narayan[31], D.I. Narrias Villar[58a], T. Naumann[42], G. Navarro[162], R. Nayyar[7], H.A. Neal[89], P.Yu. Nechaeva[96], T.J. Neep[84], P.D. Nef[143], A. Negri[121a,121b], M. Negrini[20a], S. Nektarijevic[106], C. Nellist[117], A. Nelson[163], S. Nemecek[127], P. Nemethy[110], A.A. Nepomuceno[24a], M. Nessi[30,af], M.S. Neubauer[165], M. Neumann[175], R.M. Neves[110], P. Nevski[25], P.R. Newman[18], D.H. Nguyen[6], R.B. Nickerson[120], R. Nicolaidou[136], B. Nicquevert[30], J. Nielsen[137], N. Nikiforou[35], A. Nikiforov[16], V. Nikolaenko[130,ae], I. Nikolic-Audit[80], K. Nikolopoulos[18], J.K. Nilsen[119], P. Nilsson[25], Y. Ninomiya[155], A. Nisati[132a], R. Nisius[101], T. Nobe[155], L. Nodulman[6], M. Nomachi[118], I. Nomidis[29], T. Nooney[76], S. Norberg[113], M. Nordberg[30], O. Novgorodova[44], S. Nowak[101], M. Nozaki[66], L. Nozka[115], K. Ntekas[10], E. Nurse[78], F. Nuti[88], F. O'grady[7], D.C. O'Neil[142], V. O'Shea[53], F.G. Oakham[29,d], H. Oberlack[101], T. Obermann[21], J. Ocariz[80], A. Ochi[67], I. Ochoa[35], J.P. Ochoa-Ricoux[32a], S. Oda[70], S. Odaka[66], H. Ogren[61], A. Oh[84], S.H. Oh[45], C.C. Ohm[15], H. Ohman[166], H. Oide[30], W. Okamura[118], H. Okawa[160], Y. Okumura[31], T. Okuyama[66], A. Olariu[26b], S.A. Olivares Pino[46], D. Oliveira Damazio[25], A. Olszewski[39], J. Olszowska[39], A. Onofre[126a,126e], K. Onogi[103], P.U.E. Onyisi[31,t], C.J. Oram[159a], M.J. Oreglia[31], Y. Oren[153], D. Orestano[134a,134b], N. Orlando[154], C. Oropeza Barrera[53], R.S. Orr[158], B. Osculati[50a,50b], R. Ospanov[84], G. Otero y Garzon[27], H. Otono[70], M. Ouchrif[135d], F. Ould-Saada[119], A. Ouraou[136], K.P. Oussoren[107], Q. Ouyang[33a], A. Ovcharova[15], M. Owen[53], R.E. Owen[18], V.E. Ozcan[19a], N. Ozturk[8], K. Pachal[142], A. Pacheco Pages[12], C. Padilla Aranda[12], M. Pagáčová[48], S. Pagan Griso[15], E. Paganis[139], F. Paige[25], P. Pais[86], K. Pajchel[119], G. Palacino[159b], S. Palestini[30], M. Palka[38b], D. Pallin[34], A. Palma[126a,126b], Y.B. Pan[173], E.St. Panagiotopoulou[10], C.E. Pandini[80], J.G. Panduro Vazquez[77], P. Pani[146a,146b], S. Panitkin[25], D. Pantea[26b], L. Paolozzi[49], Th.D. Papadopoulou[10], K. Papageorgiou[154], A. Paramonov[6], D. Paredes Hernandez[176], M.A. Parker[28], K.A. Parker[139], F. Parodi[50a,50b], J.A. Parsons[35], U. Parzefall[48], V. Pascuzzi[158], E. Pasqualucci[132a], S. Passaggio[50a], F. Pastore[134a,134b,*], Fr. Pastore[77], G. Pásztor[29], S. Pataraia[175], N.D. Patel[150], J.R. Pater[84], T. Pauly[30], J. Pearce[169], B. Pearson[113], L.E. Pedersen[36], M. Pedersen[119], S. Pedraza Lopez[167], R. Pedro[126a,126b],

JHEP03(2016)127

S.V. Peleganchuk[109,c], D. Pelikan[166], O. Penc[127], C. Peng[33a], H. Peng[33b], B. Penning[31], J. Penwell[61], D.V. Perepelitsa[25], E. Perez Codina[159a], M.T. Pérez García-Estañ[167], L. Perini[91a,91b], H. Pernegger[30], S. Perrella[104a,104b], R. Peschke[42], V.D. Peshekhonov[65], K. Peters[30], R.F.Y. Peters[84], B.A. Petersen[30], T.C. Petersen[36], E. Petit[42], A. Petridis[1], C. Petridou[154], P. Petroff[117], E. Petrolo[132a], F. Petrucci[134a,134b], N.E. Pettersson[157], A. Peyaud[136], R. Pezoa[32b], P.W. Phillips[131], G. Piacquadio[143], E. Pianori[170], A. Picazio[86], E. Piccaro[76], M. Piccinini[20a,20b], M.A. Pickering[120], R. Piegaia[27], D.T. Pignotti[111], J.E. Pilcher[31], A.D. Pilkington[84], A.W.J. Pin[84], J. Pina[126a,126b,126d], M. Pinamonti[164a,164c,ag], J.L. Pinfold[3], A. Pingel[36], S. Pires[80], H. Pirumov[42], M. Pitt[172], L. Plazak[144a], M.-A. Pleier[25], V. Pleskot[83], E. Plotnikova[65], P. Plucinski[146a,146b], D. Pluth[64], R. Poettgen[146a,146b], L. Poggioli[117], D. Pohl[21], G. Polesello[121a], A. Poley[42], A. Policicchio[37a,37b], R. Polifka[158], A. Polini[20a], C.S. Pollard[53], V. Polychronakos[25], K. Pommès[30], L. Pontecorvo[132a], B.G. Pope[90], G.A. Popeneciu[26c], D.S. Popovic[13], A. Poppleton[30], S. Pospisil[128], K. Potamianos[15], I.N. Potrap[65], C.J. Potter[28], C.T. Potter[116], G. Poulard[30], J. Poveda[30], V. Pozdnyakov[65], M.E. Pozo Astigarraga[30], P. Pralavorio[85], A. Pranko[15], S. Prasad[30], S. Prell[64], D. Price[84], L.E. Price[6], M. Primavera[73a], S. Prince[87], M. Proissl[46], K. Prokofiev[60c], F. Prokoshin[32b], E. Protopapadaki[136], S. Protopopescu[25], J. Proudfoot[6], M. Przybycien[38a], D. Puddu[134a,134b], E. Pueschel[86], D. Puldon[148], M. Purohit[25,ah], P. Puzo[117], J. Qian[89], G. Qin[53], Y. Qin[84], A. Quadt[54], D.R. Quarrie[15], W.B. Quayle[164a,164b], M. Queitsch-Maitland[84], D. Quilty[53], S. Raddum[119], V. Radeka[25], V. Radescu[42], S.K. Radhakrishnan[148], P. Radloff[116], P. Rados[88], F. Ragusa[91a,91b], G. Rahal[178], S. Rajagopalan[25], M. Rammensee[30], C. Rangel-Smith[166], F. Rauscher[100], S. Rave[83], T. Ravenscroft[53], M. Raymond[30], A.L. Read[119], N.P. Readioff[74], D.M. Rebuzzi[121a,121b], A. Redelbach[174], G. Redlinger[25], R. Reece[137], K. Reeves[41], L. Rehnisch[16], J. Reichert[122], H. Reisin[27], C. Rembser[30], H. Ren[33a], M. Rescigno[132a], S. Resconi[91a], O.L. Rezanova[109,c], P. Reznicek[129], R. Rezvani[95], R. Richter[101], S. Richter[78], E. Richter-Was[38b], O. Ricken[21], M. Ridel[80], P. Rieck[16], C.J. Riegel[175], J. Rieger[54], O. Rifki[113], M. Rijssenbeek[148], A. Rimoldi[121a,121b], L. Rinaldi[20a], B. Ristić[49], E. Ritsch[30], I. Riu[12], F. Rizatdinova[114], E. Rizvi[76], S.H. Robertson[87,l], A. Robichaud-Veronneau[87], D. Robinson[28], J.E.M. Robinson[42], A. Robson[53], C. Roda[124a,124b], A. Rodriguez Perez[12], S. Roe[30], C.S. Rogan[57], O. Røhne[119], A. Romaniouk[98], M. Romano[20a,20b], S.M. Romano Saez[34], E. Romero Adam[167], N. Rompotis[138], M. Ronzani[48], L. Roos[80], E. Ros[167], S. Rosati[132a], K. Rosbach[48], P. Rose[137], O. Rosenthal[141], V. Rossetti[146a,146b], E. Rossi[104a,104b], L.P. Rossi[50a], J.H.N. Rosten[28], R. Rosten[138], M. Rotaru[26b], I. Roth[172], J. Rothberg[138], D. Rousseau[117], C.R. Royon[136], A. Rozanov[85], Y. Rozen[152], X. Ruan[145c], F. Rubbo[143], I. Rubinskiy[42], V.I. Rud[99], C. Rudolph[44], M.S. Rudolph[158], F. Rühr[48], A. Ruiz-Martinez[30], Z. Rurikova[48], N.A. Rusakovich[65], A. Ruschke[100], H.L. Russell[138], J.P. Rutherfoord[7], N. Ruthmann[30], Y.F. Ryabov[123], M. Rybar[165], G. Rybkin[117], N.C. Ryder[120], A. Ryzhov[130], A.F. Saavedra[150], G. Sabato[107], S. Sacerdoti[27], H.F-W. Sadrozinski[137], R. Sadykov[65], F. Safai Tehrani[132a], P. Saha[108], M. Sahinsoy[58a], M. Saimpert[136], T. Saito[155], H. Sakamoto[155], Y. Sakurai[171], G. Salamanna[134a,134b], A. Salamon[133a], J.E. Salazar Loyola[32b], M. Saleem[113], D. Salek[107], P.H. Sales De Bruin[138], D. Salihagic[101], A. Salnikov[143], J. Salt[167], D. Salvatore[37a,37b], F. Salvatore[149], A. Salvucci[60a], A. Salzburger[30], D. Sammel[48], D. Sampsonidis[154], A. Sanchez[104a,104b], J. Sánchez[167], V. Sanchez Martinez[167], H. Sandaker[119], R.L. Sandbach[76], H.G. Sander[83], M.P. Sanders[100], M. Sandhoff[175], C. Sandoval[162], R. Sandstroem[101], D.P.C. Sankey[131], M. Sannino[50a,50b], A. Sansoni[47], C. Santoni[34], R. Santonico[133a,133b], H. Santos[126a], I. Santoyo Castillo[149], K. Sapp[125], A. Sapronov[65], J.G. Saraiva[126a,126d], B. Sarrazin[21], O. Sasaki[66], Y. Sasaki[155], K. Sato[160], G. Sauvage[5,*], E. Sauvan[5], G. Savage[77], P. Savard[158,d], C. Sawyer[131], L. Sawyer[79,p], J. Saxon[31], C. Sbarra[20a], A. Sbrizzi[20a,20b], T. Scanlon[78], D.A. Scannicchio[163], M. Scarcella[150], V. Scarfone[37a,37b],

JHEP03(2016)127

J. Schaarschmidt[172], P. Schacht[101], D. Schaefer[30], R. Schaefer[42], J. Schaeffer[83], S. Schaepe[21], S. Schaetzel[58b], U. Schäfer[83], A.C. Schaffer[117], D. Schaile[100], R.D. Schamberger[148], V. Scharf[58a], V.A. Schegelsky[123], D. Scheirich[129], M. Schernau[163], C. Schiavi[50a,50b], C. Schillo[48], M. Schioppa[37a,37b], S. Schlenker[30], K. Schmieden[30], C. Schmitt[83], S. Schmitt[58b], S. Schmitt[42], S. Schmitz[83], B. Schneider[159a], Y.J. Schnellbach[74], U. Schnoor[48], L. Schoeffel[136], A. Schoening[58b], B.D. Schoenrock[90], E. Schopf[21], A.L.S. Schorlemmer[54], M. Schott[83], D. Schouten[159a], J. Schovancova[8], S. Schramm[49], M. Schreyer[174], N. Schuh[83], M.J. Schultens[21], H.-C. Schultz-Coulon[58a], H. Schulz[16], M. Schumacher[48], B.A. Schumm[137], Ph. Schune[136], C. Schwanenberger[84], A. Schwartzman[143], T.A. Schwarz[89], Ph. Schwegler[101], H. Schweiger[84], Ph. Schwemling[136], R. Schwienhorst[90], J. Schwindling[136], T. Schwindt[21], E. Scifo[117], G. Sciolla[23], F. Scuri[124a,124b], F. Scutti[88], J. Searcy[89], P. Seema[21], S.C. Seidel[105], A. Seiden[137], F. Seifert[128], J.M. Seixas[24a], G. Sekhniaidze[104a], K. Sekhon[89], S.J. Sekula[40], D.M. Seliverstov[123,*], N. Semprini-Cesari[20a,20b], C. Serfon[30], L. Serin[117], L. Serkin[164a,164b], M. Sessa[134a,134b], R. Seuster[159a], H. Severini[113], T. Sfiligoj[75], F. Sforza[30], A. Sfyrla[49], E. Shabalina[54], L.Y. Shan[33a], R. Shang[165], J.T. Shank[22], M. Shapiro[15], P.B. Shatalov[97], K. Shaw[164a,164b], S.M. Shaw[84], A. Shcherbakova[146a,146b], C.Y. Shehu[149], P. Sherwood[78], L. Shi[151,ai], S. Shimizu[67], C.O. Shimmin[163], M. Shimojima[102], M. Shiyakova[65], A. Shmeleva[96], D. Shoaleh Saadi[95], M.J. Shochet[31], S. Shojaii[91a,91b], S. Shrestha[111], E. Shulga[98], M.A. Shupe[7], P. Sicho[127], P.E. Sidebo[147], O. Sidiropoulou[174], D. Sidorov[114], A. Sidoti[20a,20b], F. Siegert[44], Dj. Sijacki[13], J. Silva[126a,126d], S.B. Silverstein[146a], V. Simak[128], O. Simard[5], Lj. Simic[13], S. Simion[117], E. Simioni[83], B. Simmons[78], D. Simon[34], M. Simon[83], P. Sinervo[158], N.B. Sinev[116], M. Sioli[20a,20b], G. Siragusa[174], S.Yu. Sivoklokov[99], J. Sjölin[146a,146b], T.B. Sjursen[14], M.B. Skinner[72], H.P. Skottowe[57], P. Skubic[113], M. Slater[18], T. Slavicek[128], M. Slawinska[107], K. Sliwa[161], V. Smakhtin[172], B.H. Smart[46], L. Smestad[14], S.Yu. Smirnov[98], Y. Smirnov[98], L.N. Smirnova[99,aj], O. Smirnova[81], M.N.K. Smith[35], R.W. Smith[35], M. Smizanska[72], K. Smolek[128], A.A. Snesarev[96], G. Snidero[76], S. Snyder[25], R. Sobie[169,l], F. Socher[44], A. Soffer[153], D.A. Soh[151,ai], G. Sokhrannyi[75], C.A. Solans[30], M. Solar[128], J. Solc[128], E.Yu. Soldatov[98], U. Soldevila[167], A.A. Solodkov[130], A. Soloshenko[65], O.V. Solovyanov[130], V. Solovyev[123], P. Sommer[48], H.Y. Song[33b,aa], N. Soni[1], A. Sood[15], A. Sopczak[128], B. Sopko[128], V. Sopko[128], V. Sorin[12], D. Sosa[58b], C.L. Sotiropoulou[124a,124b], R. Soualah[164a,164c], A.M. Soukharev[109,c], D. South[42], B.C. Sowden[77], S. Spagnolo[73a,73b], M. Spalla[124a,124b], M. Spangenberg[170], F. Spanò[77], W.R. Spearman[57], D. Sperlich[16], F. Spettel[101], R. Spighi[20a], G. Spigo[30], L.A. Spiller[88], M. Spousta[129], R.D. St. Denis[53,*], A. Stabile[91a], S. Staerz[30], J. Stahlman[122], R. Stamen[58a], S. Stamm[16], E. Stanecka[39], R.W. Stanek[6], C. Stanescu[134a], M. Stanescu-Bellu[42], M.M. Stanitzki[42], S. Stapnes[119], E.A. Starchenko[130], G.H. Stark[31], J. Stark[55], P. Staroba[127], P. Starovoitov[58a], R. Staszewski[39], P. Steinberg[25], B. Stelzer[142], H.J. Stelzer[30], O. Stelzer-Chilton[159a], H. Stenzel[52], G.A. Stewart[53], J.A. Stillings[21], M.C. Stockton[87], M. Stoebe[87], G. Stoicea[26b], P. Stolte[54], S. Stonjek[101], A.R. Stradling[8], A. Straessner[44], M.E. Stramaglia[17], J. Strandberg[147], S. Strandberg[146a,146b], A. Strandlie[119], M. Strauss[113], P. Strizenec[144b], R. Ströhmer[174], D.M. Strom[116], R. Stroynowski[40], A. Strubig[106], S.A. Stucci[17], B. Stugu[14], N.A. Styles[42], D. Su[143], J. Su[125], R. Subramaniam[79], S. Suchek[58a], Y. Sugaya[118], M. Suk[128], V.V. Sulin[96], S. Sultansoy[4c], T. Sumida[68], S. Sun[57], X. Sun[33a], J.E. Sundermann[48], K. Suruliz[149], G. Susinno[37a,37b], M.R. Sutton[149], S. Suzuki[66], M. Svatos[127], M. Swiatlowski[31], I. Sykora[144a], T. Sykora[129], D. Ta[48], C. Taccini[134a,134b], K. Tackmann[42], J. Taenzer[158], A. Taffard[163], R. Tafirout[159a], N. Taiblum[153], H. Takai[25], R. Takashima[69], H. Takeda[67], T. Takeshita[140], Y. Takubo[66], M. Talby[85], A.A. Talyshev[109,c], J.Y.C. Tam[174], K.G. Tan[88], J. Tanaka[155], R. Tanaka[117], S. Tanaka[66], B.B. Tannenwald[111], S. Tapia Araya[32b], S. Tapprogge[83], S. Tarem[152], F. Tarrade[29], G.F. Tartarelli[91a], P. Tas[129], M. Tasevsky[127], T. Tashiro[68],

JHEP03(2016)127

E. Tassi[37a,37b], A. Tavares Delgado[126a,126b], Y. Tayalati[135d], A.C. Taylor[105], F.E. Taylor[94], G.N. Taylor[88], P.T.E. Taylor[88], W. Taylor[159b], F.A. Teischinger[30], P. Teixeira-Dias[77], K.K. Temming[48], D. Temple[142], H. Ten Kate[30], P.K. Teng[151], J.J. Teoh[118], F. Tepel[175], S. Terada[66], K. Terashi[155], J. Terron[82], S. Terzo[101], M. Testa[47], R.J. Teuscher[158,l], T. Theveneaux-Pelzer[85], J.P. Thomas[18], J. Thomas-Wilsker[77], E.N. Thompson[35], P.D. Thompson[18], R.J. Thompson[84], A.S. Thompson[53], L.A. Thomsen[176], E. Thomson[122], M. Thomson[28], M.J. Tibbetts[15], R.E. Ticse Torres[85], V.O. Tikhomirov[96,ak], Yu.A. Tikhonov[109,c], S. Timoshenko[98], E. Tiouchichine[85], P. Tipton[176], S. Tisserant[85], K. Todome[157], T. Todorov[5,*], S. Todorova-Nova[129], J. Tojo[70], S. Tokár[144a], K. Tokushuku[66], K. Tollefson[90], E. Tolley[57], L. Tomlinson[84], M. Tomoto[103], L. Tompkins[143,al], K. Toms[105], B. Tong[57], E. Torrence[116], H. Torres[142], E. Torró Pastor[138], J. Toth[85,am], F. Touchard[85], D.R. Tovey[139], T. Trefzger[174], L. Tremblet[30], A. Tricoli[30], I.M. Trigger[159a], S. Trincaz-Duvoid[80], M.F. Tripiana[12], W. Trischuk[158], B. Trocmé[55], C. Troncon[91a], M. Trottier-McDonald[15], M. Trovatelli[169], L. Truong[164a,164c], M. Trzebinski[39], A. Trzupek[39], C. Tsarouchas[30], J.C-L. Tseng[120], P.V. Tsiareshka[92], D. Tsionou[154], G. Tsipolitis[10], N. Tsirintanis[9], S. Tsiskaridze[12], V. Tsiskaridze[48], E.G. Tskhadadze[51a], K.M. Tsui[60a], I.I. Tsukerman[97], V. Tsulaia[15], S. Tsuno[66], D. Tsybychev[148], A. Tudorache[26b], V. Tudorache[26b], A.N. Tuna[57], S.A. Tupputi[20a,20b], S. Turchikhin[99,aj], D. Turecek[128], D. Turgeman[172], R. Turra[91a,91b], A.J. Turvey[40], P.M. Tuts[35], A. Tykhonov[49], M. Tylmad[146a,146b], M. Tyndel[131], I. Ueda[155], R. Ueno[29], M. Ughetto[146a,146b], F. Ukegawa[160], G. Unal[30], A. Undrus[25], G. Unel[163], F.C. Ungaro[88], Y. Unno[66], C. Unverdorben[100], J. Urban[144b], P. Urquijo[88], P. Urrejola[83], G. Usai[8], A. Usanova[62], L. Vacavant[85], V. Vacek[128], B. Vachon[87], C. Valderanis[83], N. Valencic[107], S. Valentinetti[20a,20b], A. Valero[167], L. Valery[12], S. Valkar[129], S. Vallecorsa[49], J.A. Valls Ferrer[167], W. Van Den Wollenberg[107], P.C. Van Der Deijl[107], R. van der Geer[107], H. van der Graaf[107], N. van Eldik[152], P. van Gemmeren[6], J. Van Nieuwkoop[142], I. van Vulpen[107], M.C. van Woerden[30], M. Vanadia[132a,132b], W. Vandelli[30], R. Vanguri[122], A. Vaniachine[6], F. Vannucci[80], G. Vardanyan[177], R. Vari[132a], E.W. Varnes[7], T. Varol[40], D. Varouchas[80], A. Vartapetian[8], K.E. Varvell[150], F. Vazeille[34], T. Vazquez Schroeder[87], J. Veatch[7], L.M. Veloce[158], F. Veloso[126a,126c], T. Velz[21], S. Veneziano[132a], A. Ventura[73a,73b], D. Ventura[86], M. Venturi[169], N. Venturi[158], A. Venturini[23], V. Vercesi[121a], M. Verducci[132a,132b], W. Verkerke[107], J.C. Vermeulen[107], A. Vest[44,an], M.C. Vetterli[142,d], O. Viazlo[81], I. Vichou[165], T. Vickey[139], O.E. Vickey Boeriu[139], G.H.A. Viehhauser[120], S. Viel[15], R. Vigne[62], M. Villa[20a,20b], M. Villaplana Perez[91a,91b], E. Vilucchi[47], M.G. Vincter[29], V.B. Vinogradov[65], I. Vivarelli[149], S. Vlachos[10], D. Vladoiu[100], M. Vlasak[128], M. Vogel[32a], P. Vokac[128], G. Volpi[124a,124b], M. Volpi[88], H. von der Schmitt[101], H. von Radziewski[48], E. von Toerne[21], V. Vorobel[129], K. Vorobev[98], M. Vos[167], R. Voss[30], J.H. Vossebeld[74], N. Vranjes[13], M. Vranjes Milosavljevic[13], V. Vrba[127], M. Vreeswijk[107], R. Vuillermet[30], I. Vukotic[31], Z. Vykydal[128], P. Wagner[21], W. Wagner[175], H. Wahlberg[71], S. Wahrmund[44], J. Wakabayashi[103], J. Walder[72], R. Walker[100], W. Walkowiak[141], V. Wallangen[146a,146b], C. Wang[151], F. Wang[173], H. Wang[15], H. Wang[40], J. Wang[42], J. Wang[150], K. Wang[87], R. Wang[6], S.M. Wang[151], T. Wang[21], T. Wang[35], X. Wang[176], C. Wanotayaroj[116], A. Warburton[87], C.P. Ward[28], D.R. Wardrope[78], A. Washbrook[46], P.M. Watkins[18], A.T. Watson[18], I.J. Watson[150], M.F. Watson[18], G. Watts[138], S. Watts[84], B.M. Waugh[78], S. Webb[84], M.S. Weber[17], S.W. Weber[174], J.S. Webster[6], A.R. Weidberg[120], B. Weinert[61], J. Weingarten[54], C. Weiser[48], H. Weits[107], P.S. Wells[30], T. Wenaus[25], T. Wengler[30], S. Wenig[30], N. Wermes[21], M. Werner[48], P. Werner[30], M. Wessels[58a], J. Wetter[161], K. Whalen[116], A.M. Wharton[72], A. White[8], M.J. White[1], R. White[32b], S. White[124a,124b], D. Whiteson[163], F.J. Wickens[131], W. Wiedenmann[173], M. Wielers[131], P. Wienemann[21], C. Wiglesworth[36], L.A.M. Wiik-Fuchs[21], A. Wildauer[101], H.G. Wilkens[30], H.H. Williams[122], S. Williams[107],

JHEP03(2016)127

C. Willis[90], S. Willocq[86], J.A. Wilson[18], I. Wingerter-Seez[5], F. Winklmeier[116], B.T. Winter[21], M. Wittgen[143], J. Wittkowski[100], S.J. Wollstadt[83], M.W. Wolter[39], H. Wolters[126a,126c], B.K. Wosiek[39], J. Wotschack[30], M.J. Woudstra[84], K.W. Wozniak[39], M. Wu[55], M. Wu[31], S.L. Wu[173], X. Wu[49], Y. Wu[89], T.R. Wyatt[84], B.M. Wynne[46], S. Xella[36], D. Xu[33a], L. Xu[25], B. Yabsley[150], S. Yacoob[145a], R. Yakabe[67], M. Yamada[66], D. Yamaguchi[157], Y. Yamaguchi[118], A. Yamamoto[66], S. Yamamoto[155], T. Yamanaka[155], K. Yamauchi[103], Y. Yamazaki[67], Z. Yan[22], H. Yang[33e], H. Yang[173], Y. Yang[151], Z. Yang[14], W-M. Yao[15], Y.C. Yap[80], Y. Yasu[66], E. Yatsenko[5], K.H. Yau Wong[21], J. Ye[40], S. Ye[25], I. Yeletskikh[65], A.L. Yen[57], E. Yildirim[42], K. Yorita[171], R. Yoshida[6], K. Yoshihara[122], C. Young[143], C.J.S. Young[30], S. Youssef[22], D.R. Yu[15], J. Yu[8], J.M. Yu[89], J. Yu[64], L. Yuan[67], S.P.Y. Yuen[21], A. Yurkewicz[108], I. Yusuff[28,ao], B. Zabinski[39], R. Zaidan[33d], A.M. Zaitsev[130,ae], J. Zalieckas[14], A. Zaman[148], S. Zambito[57], L. Zanello[132a,132b], D. Zanzi[88], C. Zeitnitz[175], M. Zeman[128], A. Zemla[38a], J.C. Zeng[165], Q. Zeng[143], K. Zengel[23], O. Zenin[130], T. Ženiš[144a], D. Zerwas[117], D. Zhang[89], F. Zhang[173], G. Zhang[33b,aa], H. Zhang[33c], J. Zhang[6], L. Zhang[48], R. Zhang[33b,j], X. Zhang[33d], Z. Zhang[117], X. Zhao[40], Y. Zhao[33d,117], Z. Zhao[33b], A. Zhemchugov[65], J. Zhong[120], B. Zhou[89], C. Zhou[45], L. Zhou[35], L. Zhou[40], M. Zhou[148], N. Zhou[33f], C.G. Zhu[33d], H. Zhu[33a], J. Zhu[89], Y. Zhu[33b], X. Zhuang[33a], K. Zhukov[96], A. Zibell[174], D. Zieminska[61], N.I. Zimine[65], C. Zimmermann[83], S. Zimmermann[48], Z. Zinonos[54], M. Zinser[83], M. Ziolkowski[141], L. Živković[13], G. Zobernig[173], A. Zoccoli[20a,20b], M. zur Nedden[16], G. Zurzolo[104a,104b], L. Zwalinski[30].

[1] *Department of Physics, University of Adelaide, Adelaide, Australia*
[2] *Physics Department, SUNY Albany, Albany NY, United States of America*
[3] *Department of Physics, University of Alberta, Edmonton AB, Canada*
[4] [(a)] *Department of Physics, Ankara University, Ankara;* [(b)] *Istanbul Aydin University, Istanbul;* [(c)] *Division of Physics, TOBB University of Economics and Technology, Ankara, Turkey*
[5] *LAPP, CNRS/IN2P3 and Université Savoie Mont Blanc, Annecy-le-Vieux, France*
[6] *High Energy Physics Division, Argonne National Laboratory, Argonne IL, United States of America*
[7] *Department of Physics, University of Arizona, Tucson AZ, United States of America*
[8] *Department of Physics, The University of Texas at Arlington, Arlington TX, United States of America*
[9] *Physics Department, University of Athens, Athens, Greece*
[10] *Physics Department, National Technical University of Athens, Zografou, Greece*
[11] *Institute of Physics, Azerbaijan Academy of Sciences, Baku, Azerbaijan*
[12] *Institut de Física d'Altes Energies (IFAE), The Barcelona Institute of Science and Technology, Barcelona, Spain*
[13] *Institute of Physics, University of Belgrade, Belgrade, Serbia*
[14] *Department for Physics and Technology, University of Bergen, Bergen, Norway*
[15] *Physics Division, Lawrence Berkeley National Laboratory and University of California, Berkeley CA, United States of America*
[16] *Department of Physics, Humboldt University, Berlin, Germany*
[17] *Albert Einstein Center for Fundamental Physics and Laboratory for High Energy Physics, University of Bern, Bern, Switzerland*
[18] *School of Physics and Astronomy, University of Birmingham, Birmingham, United Kingdom*
[19] [(a)] *Department of Physics, Bogazici University, Istanbul;* [(b)] *Department of Physics Engineering, Gaziantep University, Gaziantep;* [(c)] *Department of Physics, Dogus University, Istanbul, Turkey*
[20] [(a)] *INFN Sezione di Bologna;* [(b)] *Dipartimento di Fisica e Astronomia, Università di Bologna, Bologna, Italy*
[21] *Physikalisches Institut, University of Bonn, Bonn, Germany*
[22] *Department of Physics, Boston University, Boston MA, United States of America*
[23] *Department of Physics, Brandeis University, Waltham MA, United States of America*

JHEP03(2016)127

[24] [(a)] Universidade Federal do Rio De Janeiro COPPE/EE/IF, Rio de Janeiro; [(b)] Electrical Circuits Department, Federal University of Juiz de Fora (UFJF), Juiz de Fora; [(c)] Federal University of Sao Joao del Rei (UFSJ), Sao Joao del Rei; [(d)] Instituto de Fisica, Universidade de Sao Paulo, Sao Paulo, Brazil
[25] Physics Department, Brookhaven National Laboratory, Upton NY, United States of America
[26] [(a)] Transilvania University of Brasov, Brasov, Romania; [(b)] National Institute of Physics and Nuclear Engineering, Bucharest; [(c)] National Institute for Research and Development of Isotopic and Molecular Technologies, Physics Department, Cluj Napoca; [(d)] University Politehnica Bucharest, Bucharest; [(e)] West University in Timisoara, Timisoara, Romania
[27] Departamento de Física, Universidad de Buenos Aires, Buenos Aires, Argentina
[28] Cavendish Laboratory, University of Cambridge, Cambridge, United Kingdom
[29] Department of Physics, Carleton University, Ottawa ON, Canada
[30] CERN, Geneva, Switzerland
[31] Enrico Fermi Institute, University of Chicago, Chicago IL, United States of America
[32] [(a)] Departamento de Física, Pontificia Universidad Católica de Chile, Santiago; [(b)] Departamento de Física, Universidad Técnica Federico Santa María, Valparaíso, Chile
[33] [(a)] Institute of High Energy Physics, Chinese Academy of Sciences, Beijing; [(b)] Department of Modern Physics, University of Science and Technology of China, Anhui; [(c)] Department of Physics, Nanjing University, Jiangsu; [(d)] School of Physics, Shandong University, Shandong; [(e)] Department of Physics and Astronomy, Shanghai Key Laboratory for Particle Physics and Cosmology, Shanghai Jiao Tong University, Shanghai; [(f)] Physics Department, Tsinghua University, Beijing 100084, China
[34] Laboratoire de Physique Corpusculaire, Clermont Université and Université Blaise Pascal and CNRS/IN2P3, Clermont-Ferrand, France
[35] Nevis Laboratory, Columbia University, Irvington NY, United States of America
[36] Niels Bohr Institute, University of Copenhagen, Kobenhavn, Denmark
[37] [(a)] INFN Gruppo Collegato di Cosenza, Laboratori Nazionali di Frascati; [(b)] Dipartimento di Fisica, Università della Calabria, Rende, Italy
[38] [(a)] AGH University of Science and Technology, Faculty of Physics and Applied Computer Science, Krakow; [(b)] Marian Smoluchowski Institute of Physics, Jagiellonian University, Krakow, Poland
[39] Institute of Nuclear Physics Polish Academy of Sciences, Krakow, Poland
[40] Physics Department, Southern Methodist University, Dallas TX, United States of America
[41] Physics Department, University of Texas at Dallas, Richardson TX, United States of America
[42] DESY, Hamburg and Zeuthen, Germany
[43] Institut für Experimentelle Physik IV, Technische Universität Dortmund, Dortmund, Germany
[44] Institut für Kern- und Teilchenphysik, Technische Universität Dresden, Dresden, Germany
[45] Department of Physics, Duke University, Durham NC, United States of America
[46] SUPA - School of Physics and Astronomy, University of Edinburgh, Edinburgh, United Kingdom
[47] INFN Laboratori Nazionali di Frascati, Frascati, Italy
[48] Fakultät für Mathematik und Physik, Albert-Ludwigs-Universität, Freiburg, Germany
[49] Section de Physique, Université de Genève, Geneva, Switzerland
[50] [(a)] INFN Sezione di Genova; [(b)] Dipartimento di Fisica, Università di Genova, Genova, Italy
[51] [(a)] E. Andronikashvili Institute of Physics, Iv. Javakhishvili Tbilisi State University, Tbilisi; [(b)] High Energy Physics Institute, Tbilisi State University, Tbilisi, Georgia
[52] II Physikalisches Institut, Justus-Liebig-Universität Giessen, Giessen, Germany
[53] SUPA - School of Physics and Astronomy, University of Glasgow, Glasgow, United Kingdom
[54] II Physikalisches Institut, Georg-August-Universität, Göttingen, Germany
[55] Laboratoire de Physique Subatomique et de Cosmologie, Université Grenoble-Alpes, CNRS/IN2P3, Grenoble, France
[56] Department of Physics, Hampton University, Hampton VA, United States of America
[57] Laboratory for Particle Physics and Cosmology, Harvard University, Cambridge MA, United States of America

JHEP03(2016)127

[58] [(a)] Kirchhoff-Institut für Physik, Ruprecht-Karls-Universität Heidelberg, Heidelberg; [(b)] Physikalisches Institut, Ruprecht-Karls-Universität Heidelberg, Heidelberg; [(c)] ZITI Institut für technische Informatik, Ruprecht-Karls-Universität Heidelberg, Mannheim, Germany
[59] Faculty of Applied Information Science, Hiroshima Institute of Technology, Hiroshima, Japan
[60] [(a)] Department of Physics, The Chinese University of Hong Kong, Shatin, N.T., Hong Kong; [(b)] Department of Physics, The University of Hong Kong, Hong Kong; [(c)] Department of Physics, The Hong Kong University of Science and Technology, Clear Water Bay, Kowloon, Hong Kong, China
[61] Department of Physics, Indiana University, Bloomington IN, United States of America
[62] Institut für Astro- und Teilchenphysik, Leopold-Franzens-Universität, Innsbruck, Austria
[63] University of Iowa, Iowa City IA, United States of America
[64] Department of Physics and Astronomy, Iowa State University, Ames IA, United States of America
[65] Joint Institute for Nuclear Research, JINR Dubna, Dubna, Russia
[66] KEK, High Energy Accelerator Research Organization, Tsukuba, Japan
[67] Graduate School of Science, Kobe University, Kobe, Japan
[68] Faculty of Science, Kyoto University, Kyoto, Japan
[69] Kyoto University of Education, Kyoto, Japan
[70] Department of Physics, Kyushu University, Fukuoka, Japan
[71] Instituto de Física La Plata, Universidad Nacional de La Plata and CONICET, La Plata, Argentina
[72] Physics Department, Lancaster University, Lancaster, United Kingdom
[73] [(a)] INFN Sezione di Lecce; [(b)] Dipartimento di Matematica e Fisica, Università del Salento, Lecce, Italy
[74] Oliver Lodge Laboratory, University of Liverpool, Liverpool, United Kingdom
[75] Department of Physics, Jožef Stefan Institute and University of Ljubljana, Ljubljana, Slovenia
[76] School of Physics and Astronomy, Queen Mary University of London, London, United Kingdom
[77] Department of Physics, Royal Holloway University of London, Surrey, United Kingdom
[78] Department of Physics and Astronomy, University College London, London, United Kingdom
[79] Louisiana Tech University, Ruston LA, United States of America
[80] Laboratoire de Physique Nucléaire et de Hautes Energies, UPMC and Université Paris-Diderot and CNRS/IN2P3, Paris, France
[81] Fysiska institutionen, Lunds universitet, Lund, Sweden
[82] Departamento de Fisica Teorica C-15, Universidad Autonoma de Madrid, Madrid, Spain
[83] Institut für Physik, Universität Mainz, Mainz, Germany
[84] School of Physics and Astronomy, University of Manchester, Manchester, United Kingdom
[85] CPPM, Aix-Marseille Université and CNRS/IN2P3, Marseille, France
[86] Department of Physics, University of Massachusetts, Amherst MA, United States of America
[87] Department of Physics, McGill University, Montreal QC, Canada
[88] School of Physics, University of Melbourne, Victoria, Australia
[89] Department of Physics, The University of Michigan, Ann Arbor MI, United States of America
[90] Department of Physics and Astronomy, Michigan State University, East Lansing MI, United States of America
[91] [(a)] INFN Sezione di Milano; [(b)] Dipartimento di Fisica, Università di Milano, Milano, Italy
[92] B.I. Stepanov Institute of Physics, National Academy of Sciences of Belarus, Minsk, Republic of Belarus
[93] National Scientific and Educational Centre for Particle and High Energy Physics, Minsk, Republic of Belarus
[94] Department of Physics, Massachusetts Institute of Technology, Cambridge MA, United States of America
[95] Group of Particle Physics, University of Montreal, Montreal QC, Canada
[96] P.N. Lebedev Physical Institute of the Russian Academy of Sciences, Moscow, Russia
[97] Institute for Theoretical and Experimental Physics (ITEP), Moscow, Russia
[98] National Research Nuclear University MEPhI, Moscow, Russia
[99] D.V. Skobeltsyn Institute of Nuclear Physics, M.V. Lomonosov Moscow State University, Moscow, Russia

JHEP03(2016)127

[100] Fakultät für Physik, Ludwig-Maximilians-Universität München, München, Germany
[101] Max-Planck-Institut für Physik (Werner-Heisenberg-Institut), München, Germany
[102] Nagasaki Institute of Applied Science, Nagasaki, Japan
[103] Graduate School of Science and Kobayashi-Maskawa Institute, Nagoya University, Nagoya, Japan
[104] [(a)] INFN Sezione di Napoli; [(b)] Dipartimento di Fisica, Università di Napoli, Napoli, Italy
[105] Department of Physics and Astronomy, University of New Mexico, Albuquerque NM, United States of America
[106] Institute for Mathematics, Astrophysics and Particle Physics, Radboud University Nijmegen/Nikhef, Nijmegen, Netherlands
[107] Nikhef National Institute for Subatomic Physics and University of Amsterdam, Amsterdam, Netherlands
[108] Department of Physics, Northern Illinois University, DeKalb IL, United States of America
[109] Budker Institute of Nuclear Physics, SB RAS, Novosibirsk, Russia
[110] Department of Physics, New York University, New York NY, United States of America
[111] Ohio State University, Columbus OH, United States of America
[112] Faculty of Science, Okayama University, Okayama, Japan
[113] Homer L. Dodge Department of Physics and Astronomy, University of Oklahoma, Norman OK, United States of America
[114] Department of Physics, Oklahoma State University, Stillwater OK, United States of America
[115] Palacký University, RCPTM, Olomouc, Czech Republic
[116] Center for High Energy Physics, University of Oregon, Eugene OR, United States of America
[117] LAL, Univ. Paris-Sud, CNRS/IN2P3, Université Paris-Saclay, Orsay, France
[118] Graduate School of Science, Osaka University, Osaka, Japan
[119] Department of Physics, University of Oslo, Oslo, Norway
[120] Department of Physics, Oxford University, Oxford, United Kingdom
[121] [(a)] INFN Sezione di Pavia; [(b)] Dipartimento di Fisica, Università di Pavia, Pavia, Italy
[122] Department of Physics, University of Pennsylvania, Philadelphia PA, United States of America
[123] National Research Centre "Kurchatov Institute" B.P.Konstantinov Petersburg Nuclear Physics Institute, St. Petersburg, Russia
[124] [(a)] INFN Sezione di Pisa; [(b)] Dipartimento di Fisica E. Fermi, Università di Pisa, Pisa, Italy
[125] Department of Physics and Astronomy, University of Pittsburgh, Pittsburgh PA, United States of America
[126] [(a)] Laboratório de Instrumentação e Física Experimental de Partículas - LIP, Lisboa; [(b)] Faculdade de Ciências, Universidade de Lisboa, Lisboa; [(c)] Department of Physics, University of Coimbra, Coimbra; [(d)] Centro de Física Nuclear da Universidade de Lisboa, Lisboa; [(e)] Departamento de Fisica, Universidade do Minho, Braga; [(f)] Departamento de Fisica Teorica y del Cosmos and CAFPE, Universidad de Granada, Granada (Spain); [(g)] Dep Fisica and CEFITEC of Faculdade de Ciencias e Tecnologia, Universidade Nova de Lisboa, Caparica, Portugal
[127] Institute of Physics, Academy of Sciences of the Czech Republic, Praha, Czech Republic
[128] Czech Technical University in Prague, Praha, Czech Republic
[129] Faculty of Mathematics and Physics, Charles University in Prague, Praha, Czech Republic
[130] State Research Center Institute for High Energy Physics (Protvino), NRC KI, Russia
[131] Particle Physics Department, Rutherford Appleton Laboratory, Didcot, United Kingdom
[132] [(a)] INFN Sezione di Roma; [(b)] Dipartimento di Fisica, Sapienza Università di Roma, Roma, Italy
[133] [(a)] INFN Sezione di Roma Tor Vergata; [(b)] Dipartimento di Fisica, Università di Roma Tor Vergata, Roma, Italy
[134] [(a)] INFN Sezione di Roma Tre; [(b)] Dipartimento di Matematica e Fisica, Università Roma Tre, Roma, Italy
[135] [(a)] Faculté des Sciences Ain Chock, Réseau Universitaire de Physique des Hautes Energies - Université Hassan II, Casablanca; [(b)] Centre National de l'Energie des Sciences Techniques Nucleaires, Rabat; [(c)] Faculté des Sciences Semlalia, Université Cadi Ayyad, LPHEA-Marrakech; [(d)] Faculté des Sciences, Université Mohamed Premier and LPTPM, Oujda; [(e)] Faculté des sciences, Université Mohammed V, Rabat, Morocco

JHEP03(2016)127

[136] DSM/IRFU (Institut de Recherches sur les Lois Fondamentales de l'Univers), CEA Saclay (Commissariat à l'Energie Atomique et aux Energies Alternatives), Gif-sur-Yvette, France
[137] Santa Cruz Institute for Particle Physics, University of California Santa Cruz, Santa Cruz CA, United States of America
[138] Department of Physics, University of Washington, Seattle WA, United States of America
[139] Department of Physics and Astronomy, University of Sheffield, Sheffield, United Kingdom
[140] Department of Physics, Shinshu University, Nagano, Japan
[141] Fachbereich Physik, Universität Siegen, Siegen, Germany
[142] Department of Physics, Simon Fraser University, Burnaby BC, Canada
[143] SLAC National Accelerator Laboratory, Stanford CA, United States of America
[144] [(a)] Faculty of Mathematics, Physics & Informatics, Comenius University, Bratislava; [(b)] Department of Subnuclear Physics, Institute of Experimental Physics of the Slovak Academy of Sciences, Kosice, Slovak Republic
[145] [(a)] Department of Physics, University of Cape Town, Cape Town; [(b)] Department of Physics, University of Johannesburg, Johannesburg; [(c)] School of Physics, University of the Witwatersrand, Johannesburg, South Africa
[146] [(a)] Department of Physics, Stockholm University; [(b)] The Oskar Klein Centre, Stockholm, Sweden
[147] Physics Department, Royal Institute of Technology, Stockholm, Sweden
[148] Departments of Physics & Astronomy and Chemistry, Stony Brook University, Stony Brook NY, United States of America
[149] Department of Physics and Astronomy, University of Sussex, Brighton, United Kingdom
[150] School of Physics, University of Sydney, Sydney, Australia
[151] Institute of Physics, Academia Sinica, Taipei, Taiwan
[152] Department of Physics, Technion: Israel Institute of Technology, Haifa, Israel
[153] Raymond and Beverly Sackler School of Physics and Astronomy, Tel Aviv University, Tel Aviv, Israel
[154] Department of Physics, Aristotle University of Thessaloniki, Thessaloniki, Greece
[155] International Center for Elementary Particle Physics and Department of Physics, The University of Tokyo, Tokyo, Japan
[156] Graduate School of Science and Technology, Tokyo Metropolitan University, Tokyo, Japan
[157] Department of Physics, Tokyo Institute of Technology, Tokyo, Japan
[158] Department of Physics, University of Toronto, Toronto ON, Canada
[159] [(a)] TRIUMF, Vancouver BC; [(b)] Department of Physics and Astronomy, York University, Toronto ON, Canada
[160] Faculty of Pure and Applied Sciences, and Center for Integrated Research in Fundamental Science and Engineering, University of Tsukuba, Tsukuba, Japan
[161] Department of Physics and Astronomy, Tufts University, Medford MA, United States of America
[162] Centro de Investigaciones, Universidad Antonio Narino, Bogota, Colombia
[163] Department of Physics and Astronomy, University of California Irvine, Irvine CA, United States of America
[164] [(a)] INFN Gruppo Collegato di Udine, Sezione di Trieste, Udine; [(b)] ICTP, Trieste; [(c)] Dipartimento di Chimica, Fisica e Ambiente, Università di Udine, Udine, Italy
[165] Department of Physics, University of Illinois, Urbana IL, United States of America
[166] Department of Physics and Astronomy, University of Uppsala, Uppsala, Sweden
[167] Instituto de Física Corpuscular (IFIC) and Departamento de Física Atómica, Molecular y Nuclear and Departamento de Ingeniería Electrónica and Instituto de Microelectrónica de Barcelona (IMB-CNM), University of Valencia and CSIC, Valencia, Spain
[168] Department of Physics, University of British Columbia, Vancouver BC, Canada
[169] Department of Physics and Astronomy, University of Victoria, Victoria BC, Canada
[170] Department of Physics, University of Warwick, Coventry, United Kingdom
[171] Waseda University, Tokyo, Japan
[172] Department of Particle Physics, The Weizmann Institute of Science, Rehovot, Israel

JHEP03(2016)127

[173] Department of Physics, University of Wisconsin, Madison WI, United States of America
[174] Fakultät für Physik und Astronomie, Julius-Maximilians-Universität, Würzburg, Germany
[175] Fakult[a]t für Mathematik und Naturwissenschaften, Fachgruppe Physik, Bergische Universität Wuppertal, Wuppertal, Germany
[176] Department of Physics, Yale University, New Haven CT, United States of America
[177] Yerevan Physics Institute, Yerevan, Armenia
[178] Centre de Calcul de l'Institut National de Physique Nucléaire et de Physique des Particules (IN2P3), Villeurbanne, France

[a] Also at Department of Physics, King's College London, London, United Kingdom
[b] Also at Institute of Physics, Azerbaijan Academy of Sciences, Baku, Azerbaijan
[c] Also at Novosibirsk State University, Novosibirsk, Russia
[d] Also at TRIUMF, Vancouver BC, Canada
[e] Also at Department of Physics & Astronomy, University of Louisville, Louisville, KY, United States of America
[f] Also at Department of Physics, California State University, Fresno CA, United States of America
[g] Also at Department of Physics, University of Fribourg, Fribourg, Switzerland
[h] Also at Departamento de Fisica e Astronomia, Faculdade de Ciencias, Universidade do Porto, Portugal
[i] Also at Tomsk State University, Tomsk, Russia
[j] Also at CPPM, Aix-Marseille Université and CNRS/IN2P3, Marseille, France
[k] Also at Universita di Napoli Parthenope, Napoli, Italy
[l] Also at Institute of Particle Physics (IPP), Canada
[m] Also at Particle Physics Department, Rutherford Appleton Laboratory, Didcot, United Kingdom
[n] Also at Department of Physics, St. Petersburg State Polytechnical University, St. Petersburg, Russia
[o] Also at Department of Physics, The University of Michigan, Ann Arbor MI, United States of America
[p] Also at Louisiana Tech University, Ruston LA, United States of America
[q] Also at Institucio Catalana de Recerca i Estudis Avancats, ICREA, Barcelona, Spain
[r] Also at Graduate School of Science, Osaka University, Osaka, Japan
[s] Also at Department of Physics, National Tsing Hua University, Taiwan
[t] Also at Department of Physics, The University of Texas at Austin, Austin TX, United States of America
[u] Also at Institute of Theoretical Physics, Ilia State University, Tbilisi, Georgia
[v] Also at CERN, Geneva, Switzerland
[w] Also at Georgian Technical University (GTU),Tbilisi, Georgia
[x] Also at Ochadai Academic Production, Ochanomizu University, Tokyo, Japan
[y] Also at Manhattan College, New York NY, United States of America
[z] Also at Hellenic Open University, Patras, Greece
[aa] Also at Institute of Physics, Academia Sinica, Taipei, Taiwan
[ab] Also at LAL, Univ. Paris-Sud, CNRS/IN2P3, Université Paris-Saclay, Orsay, France
[ac] Also at Academia Sinica Grid Computing, Institute of Physics, Academia Sinica, Taipei, Taiwan
[ad] Also at School of Physics, Shandong University, Shandong, China
[ae] Also at Moscow Institute of Physics and Technology State University, Dolgoprudny, Russia
[af] Also at section de Physique, Université de Genève, Geneva, Switzerland
[ag] Also at International School for Advanced Studies (SISSA), Trieste, Italy
[ah] Also at Department of Physics and Astronomy, University of South Carolina, Columbia SC, United States of America
[ai] Also at School of Physics and Engineering, Sun Yat-sen University, Guangzhou, China
[aj] Also at Faculty of Physics, M.V.Lomonosov Moscow State University, Moscow, Russia
[ak] Also at National Research Nuclear University MEPhI, Moscow, Russia

JHEP03(2016)127

[al] Also at Department of Physics, Stanford University, Stanford CA, United States of America
[am] Also at Institute for Particle and Nuclear Physics, Wigner Research Centre for Physics, Budapest, Hungary
[an] Also at Flensburg University of Applied Sciences, Flensburg, Germany
[ao] Also at University of Malaya, Department of Physics, Kuala Lumpur, Malaysiay
[*] Deceased

JHEP03(2016)127